Design and implementation of a cuvette system for light analysis of photosynthetic pigments

Ahmed Bassam Mahmoud

Department of Bioresource Engineering

McGill University

Montreal, Quebec, Canada

A thesis submitted to McGill University in partial fulfillment of the requirements of the degree of Master of Science

January, 2021

Abstract

Studying photosynthetic pigments is essential in understanding the mechanisms of photosynthesis; an important aspect of this is the examination of the absorption characteristics of these pigments, and the nature of their interaction with light. The need and requirements of a modular, flexible cuvette system were investigated by performing light absorption tests with photosynthetic pigments. A proposed in-house design was conceived and implemented after determining the appropriate requirements and dimensions of the system by running tests with a commercial spectrometer and with the LED light sources and spectroradiometer readily available at McGill University to maximize compatibility and reduce the cost of the new system. A series of tests were performed using blank mineral oil and water samples, and two types of glass cuvettes with the new system. The angles of light incidence were varied, with each combination of solvent and cuvette undergoing testing at vertical and horizontal angles, in addition to four other angles. The obtained results show the occurrence of a lensing effect; this effect amplifies light intensity, and is influenced by the shape and material of the cuvette container, the type of solvent used, and the tested angle of incidence. The cylindrical shape of the cuvette combined with a mineral oil sample results in a high and significant increase lensing, while the rectangular cuvette shows some amplification when using water based sample. The building procedure and results of the new system, as well as the recommendation for future improvements are detailed in this thesis.

Résumé

L'étude des pigments photosynthétiques est essentielle pour comprendre les mécanismes de la photosynthèse. Un aspect important de cette étude est l'examen des caractéristiques d'absorption de ces pigments, et la nature de leur interaction avec la lumière. Le besoin et les exigences d'un système de cuvettes modulaire et flexible ont été étudiés en effectuant des tests d'absorption de lumière avec des pigments photosynthétiques. Une proposition de conception interne a été conçue et mise en œuvre après avoir déterminé les exigences et les dimensions appropriées du système en effectuant des tests avec un spectromètre commercial et avec les sources de lumière LED et le spectroradiomètre facilement disponibles dans le laboratoire de production de biomasse afin de maximiser la compatibilité et de réduire le coût du nouveau système. Une série de tests a été réalisée en utilisant des échantillons vierges d'huile minérale et d'eau, ainsi que deux types de cuvettes en verre avec le nouveau système. Les angles d'incidence de la lumière ont également été variés, chaque combinaison de solvant et de cuvette ayant été testée à des angles verticaux et horizontaux, ainsi qu'à quatre autres angles intermédiaires. Les résultats obtenus montrent l'apparition d'un effet de lentille ; cet effet amplifie l'intensité de la lumière et est influencé par la forme et le matériau du récipient de la cuvette, le type de solvant utilisé et l'angle d'incidence testé. La forme cylindrique de la cuvette combinée à un échantillon d'huile minérale entraîne une augmentation élevée et significative de l'effet de lentille, tandis que la cuvette rectangulaire montre une certaine amplification lors de l'utilisation d'un échantillon à base d'eau. La procédure de construction et

les résultats du nouveau système, ainsi que les recommandations pour de futures améliorations sont détaillées dans cette thèse.

ACKNOWLEDGEMENT

I extend my deepest gratitude to Dr. Mark Lefsrud for his support over the course of this degree. I thank Dr. Valérie Orsat for her wise and valuable advice. I also thank Mr. Scott Manktelow and Bo-Sen Wu for their selfless and essential advice and help, without which this project would not have been completed.

Last but not least, I thank my family for everything, especially my father, mother, and grandmother. I will never forget the sacrifices you made for me, and will always be in your debt.

Table of Contents

Table of Figures

CONTRIBUTION OF AUTHORS

The design of the experiment was completed by Ahmed Mahmoud and Dr Mark Lefsrud.

The construction and testing of the apparatus was completed by Ahmed Mahmoud.

The analysis and writing was completed by Ahmed Mahmoud.

The LED Light source and spectroradiometer setups were done by Bo-Sen Wu.

Mr. Scott Manktelow helped with machine operation and knowledge transfer in the workshop.

Abbreviations

RQE: Relative Quantum Efficiency

TIR: Total Internal Reflection

COB: Chip on Board

HID: High-intensity discharge

LED: Light Emitting Diode

PAR: Photosynthetic Active Radiation

Chl: Chlorophyll

PPFD: Photosynthetic Photon Flux Density

1. Chapter 1: Literature Review

1.1. Main Photosynthetic Pigments and their Light Absorbance

Plants perform photosynthesis by utilizing a group of pigments which absorb and transfer light energy to the photosynthetic reaction complexes (Cooper, 2000; Mishra, 2004). These photosynthetic pigments form the two membrane protein complexes Photosystem I and Photosystem II, and are categorized as either chlorophyll pigments or carotenoid pigments (Cooper, 2000; Mishra, 2004). Chlorophyll pigments include chlorophyll a (chl a) and chlorophyll b (chl b) (Lockstein et al., 2007). While carotenoid include β-carotene, and carotenoid subset xanthophylls including lutein, violaxanthin, anteroxanthin and zeaxanthin (Sandmann, 2001, Demmig-Adams et al., 1996).

The most abundant of these pigments is chl a, which is present in the light reaction centers of all photosynthetic organisms (Farabee, 2007), and is the reaction driving pigment in Photosystem I and Photosystem II complexes. Chl b and carotenoids are found in higher plants, and are referred to as secondary pigments. Secondary pigments surround the light reaction centers in order to collect and deliver light energy through resonance energy transfer to chl a, which exists inside the reaction centers. Carotenoids act as a defense mechanism by dissipating excess energy, thus preventing damage to the photosynthetic apparatus (Frank and Cogdell, 1996), and they inhibit oxidative damage by binding reactive singlet oxygen (Demmig-Adams et al., 1996).

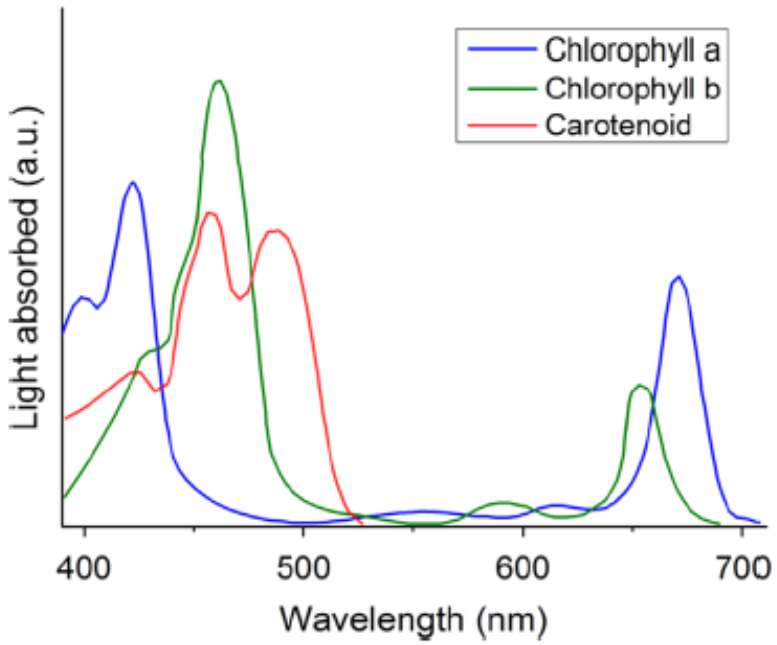

Figure 1: Absorption spectrum of chlorophyll and antenna pigments (Singh et al., 2015)

Photosynthetic pigments each have a pattern of light absorption; this pattern is known as the absorption spectrum, shown in Figure 1 (Singh et al., 2015). It represents the relative absorption of specific light wavelengths for a given pigment, and is dictated by the molecular structure of the pigment (Wozniak et al., 2007). The molecular structure of chlorophyll includes a porphyrin ring while carotenoids possess a carbon ring. The presence of relatively unstable double bonds enables the pigments to absorb and transfer the energy of photons through electron transition which in turn transfers photon energy (Wozniak et al., 2007). Energy transfer between pigment molecules is done via fluorescent resonance energy transfer, with certain wavelengths resulting in more resonance and therefore energy transfer than others (Cohen et al., 2002).

For chlorophyll, absorption peaks are in the red and blue region of visible light, with chl a dissolved in acetone having peaks at 430 and 663 nm, while chl b in acetone has its absorption peaks at 453 and 642 nm (Taiz and Zeiger, 1998). Absorption of β-carotene and lutein is strongest in the blue region of visible light, with β-carotene in acetone having its maximum

peak at 454 nm, and lutein in acetone having its maximum peak at 448 nm (Hopkins and Huner, 2004; Köst, 1988; Taiz and Zeiger, 1998). β-carotene and lutein have local absorption peaks at 477 nm for β-carotene, and 2 local absorption peaks at 422 and 474 nm for lutein. Absorption peaks can shift in response to the surrounding conditions of the chloroplasts by up to 38 nm in plants (Heber and Shuvalov, 2005).

The absorption characteristic of chlorophyll; which peaks in the red and blue region of visible light spectrum, gives it a green appearance (Lockstein et al., 2007). Chl a is the most abundant pigment in all photosynthetic organisms (Farabee, 2007) and acts as the primary electron donor in Photosystem I and Photosystem II complexes, while chl b is available in higher plants as a secondary pigment (Lockstein et al., 2007). Chlorophyll molecules have a porphyrin ring in their chemical composition, with the difference between chl a and chl b being that a molecule of chl a has a methyl group, while a molecule of chl b has a formyl group, this difference in molecular structure results in a notable variation in the absorption properties of the two main chlorophyll pigments, which in turn extends the overall absorption spectrum of higher plants (Scheer, 2006). The bonds between chlorophyll molecules and chloroplast proteins are non-covalent, and together they form a protein-chlorophyll complex (Lockstein et al., 2007).

Carotenoids are secondary pigments and they typically have a red, orange or yellow appearance, since their absorption is strongest in the blue region of visible light (Lockstein et al., 2007; Taiz and Zeiger, 1998) and form a complex antenna network in the thylakoid membrane that transfers energy to and from the reaction centers via resonant energy transfer (Lockstein et al., 2007; Cogdell, 1978). Carotenoid molecules consist of a polyene chain of double bonds with a varying length and possible carbon rings at the ends of the chain, depending on the type of carotenoid (Vershinin, 1999). Carotenoids can transfer energy to chlorophyll through singlet-singlet energy transfer, which enables it to act as an antenna system to absorb and deliver light energy to the reaction centers during photosynthesis (Cogdell, 1978). Carotenoids can also transfer excess energy from chlorophyll through triplet-triplet energy transfer; this enables them to perform a photo-protective role in plants (Cogdell, 1978). Chlorophylls and carotenoids

are therefore able to absorb and transfer light energy due to the conjugated nature of bonds in their molecular structure (Wozniak et al., 2007).

Plant photosynthetic utilization of light energy peaks in the red and blue region of visible light, where chlorophyll has its own absorption peaks. However, the fluorescence characteristics of chl a facilitates efficient transfer of excitation energy from secondary pigments to the reaction centers where chl a exists. This effectively extends the range of light energy utilization for photosynthesis by plants beyond the absorbance peaks of the dominant chlorophyll (Frank and Cogdell, 1996; Koning, 1994; Young, 1991). Photosynthetic pigments play a protective role against potentially hazardous complications caused by extremely high irradiance (Frank and Cogdell, 1996; Demmig-Adams et al., 1996). This can be done by storing excess energy in the form of excited, singlet Chl *a* ($^1Chl^*$) molecules in the reaction centers (Müller et al, 2001). Moreover, the oxygenated carotenoid xanthophyll pigments, specifically violaxanthin, antheraxanthin, and zeaxanthin can thermally dissipate excess energy in the reaction centers, preventing photo-oxidative damage to the photosynthetic apparatus. Violaxanthin, antheraxanthin and zeaxanthin scavenge for evolved singlet-oxygen (1O2), an oxidizing agent that is hazardous for the plant due to its high reactivity which can cause cell damage by oxidizing lipids, proteins and pigments. This damage can photo-inhibit the photosystem light harvesting centers, can cause photo-bleaching, and eventually the death of the plant (Demmig-Adams and Adams, 1992; Mozzo, 2008; Müller et al, 2001).

1.2. Introduction to LEDs

LEDs are a promising source of electrical light for controlled environment agriculture (CEA) plant production and research, compared to traditional electrical lighting sources (Massa et al., 2008; Morrow, 2008). The benefits of using LEDs include light beam controllability, low heat emission in the direction of illumination, and wavelength option flexibility (Massa et al., 2015; Morrow, 2008; Yeh and Chung, 2009). LEDs have a narrow band light emission spectrum, and

can produce a higher irradiance of isolated wavelengths of light than monochromatic light previously obtained through filters, which in turn allows more accurate assessments of plant physiological responses to them (Lefsrud, 2008). The use of LEDs can have a higher initial capital cost, compared to traditional sources of horticultural lighting (Singh et al., 2015). Economic analysis indicates that LEDs can reduce the electricity cost and investment will be returned in long-term operations in green house industries, as shown in Figure 2 (Singh et al., 2015).

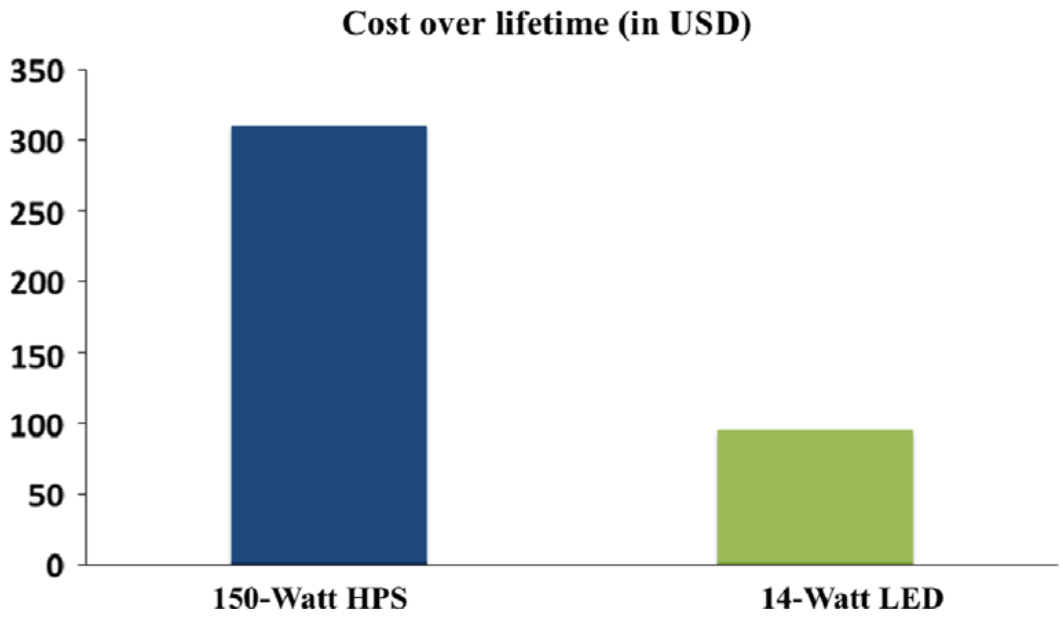

Figure 2: Lifetime cost comparison of a 150-W HPS lamp and a 14-W LED, (Singh et al., 2015)

Subjecting plants to specific wavelengths of light, individually or in addition to traditional horticultural lighting, can have a great effect on the plant, and can increase the nutrient content of the end product (Singh et al., 2015). This positions LEDs as a the top choice ~~for~~ of electrical horticultural light options for growers seeking an efficient, flexible source of light, with enhanced nutrient content, and for researchers seeking to explore the benefits of using specific wavelengths of light on plant physiology and characteristics.

1.3. LED properties

Light emitting diodes (LED), are optoelectronic semiconductors, consisting of a PN-junction (Holonyak Jr and Bevacqua, 1962). These devices are formed by doping the junction with chemical impurities to create a positive part and a negative part, which are then placed side by side to generate light (Holonyac et al. 1962; Lafont et al., 2012). The N side of the junction is a donor of electrons and is doped with impurity material having an excess of valence electrons available for conduction, while the P side is a donor of holes, or acceptor of electrons, and is doped with an impurity material having a shortage of electrons (Kasap, 2001). When no electric potential is applied to the junction, it is said to be at zero-bias, and neither electrons move from the N to the P regions nor holes from the P to N region (Kasap, 2001) as shown in Figure 3 (retrieved from www.physics-and-radio-electronics.com).

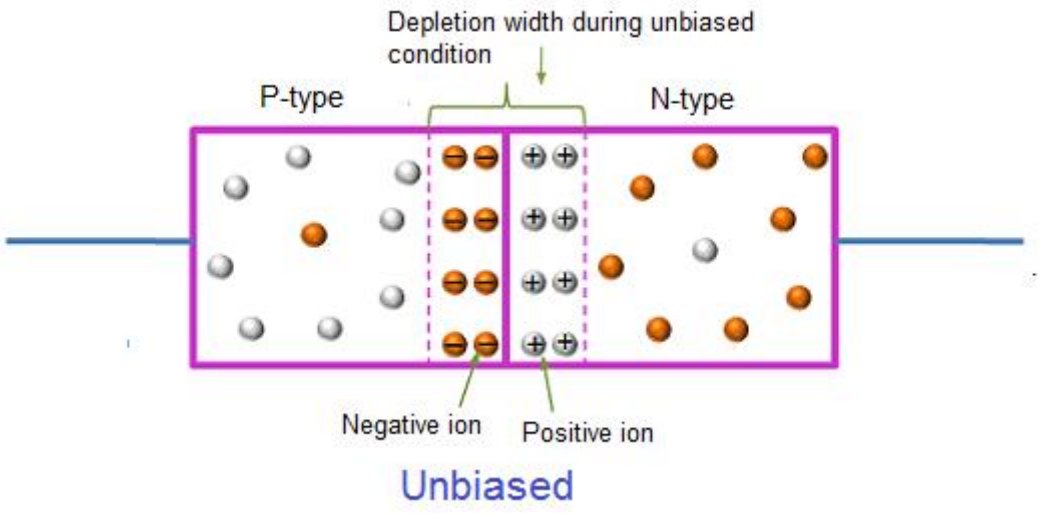

Figure 3: PN junction without an applied electric potential

If the junction is placed in a circuit with positive potential applied to the P side of the junction and negative potential applied to the N side of the junction, it is said to be in forward bias, under forward bias, free electrons and holes can gain sufficient energy to cross the barrier between the two regions (enter into the depletion region)(Kasap, 2001). Hence the width of the separating depletion region is reduced and the potential barrier between the two junctions is

narrowed (Kasap, 2001). When a free electron meets a free hole in the junction (at the depletion region) recombination happens. During recombination, when electrons find vacant states of lower energy level in the holes, they move from the conduction band to fill holes in the valence band, which is of a lower energy level (Singh et al., 2015). The difference of energy is emitted as a photon and optical energy is released that is determined by the material of the PN junction (Yeh and Chung, 2009) as illustrated in Figure 4 (retrieved from www.physics-and-radio-electronics.com).

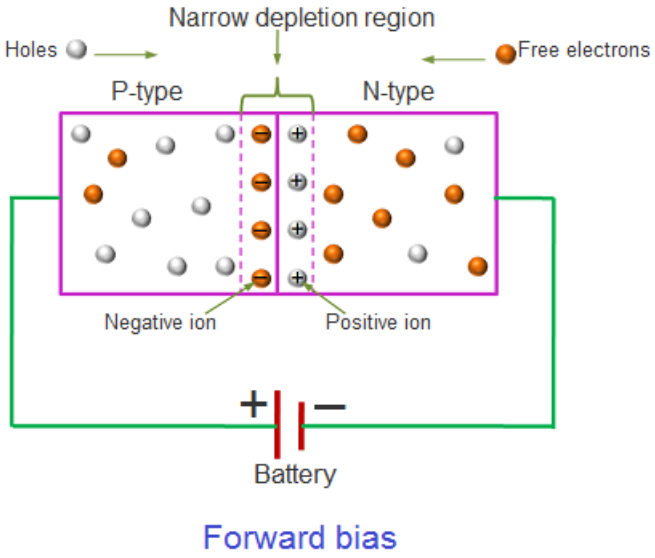

Figure 4: PN-junction in forward bias

This difference in energy, between the energy of the free electrons moving from the N side of the junction (conduction band), and the valence energy of the holes moving from the P side of the junction (valence band) is known as the band gap (Kasap, 2001). The band gap energy is equal to the energy of the photons released and therefore determines the frequency and wavelength of light emission. This wavelength has a mathematical relation to the band gap energy (Kasap, 2001).

$$\lambda = \frac{hc}{E_g} = \frac{1.24}{E_g}\ \mu m$$

Equation 1

Where h is Planck's constant, c is the speed of the light, and Eg is the band gap in electron Volts (eV)

In order to tune the wavelength of the resulting light, the band gap energy is manipulated. This is done by changing the doping material in the junction (Kasap, 2001), and its concentrations (Yufeng et al., 2007). This is because the bonds formed in the solid substrate of the junction cause the formation of delocalized molecular orbitals (Kasap, 2001). Therefore changes to the chemical composition of the junction medium also changes the energy levels of the delocalized molecular orbitals of the P and N sides of the junction, which in turn changes the band gap energy. Charge carrier concentration along the profile of a PN-junction is shown in Figure 5 (Kasap, 2001).

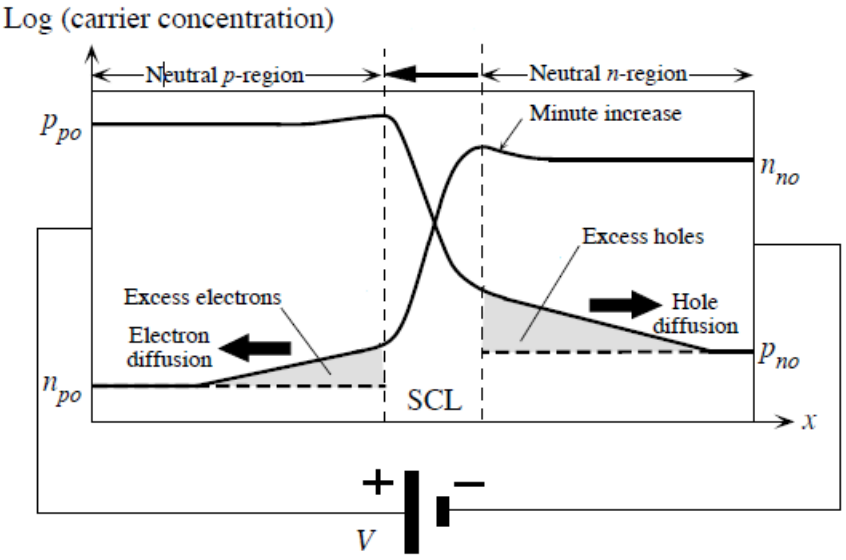

Figure 5: Carrier concentration of a forward biased PN junction. "po" is the charge carrier concentrations for holes, while "no" is that of electrons. SCL stands for the space charge layer, or the depletion region (Kasap, 2001).

Doping material used to produce red light can be a combination of aluminum gallium arsenide (AlGaAs), gallium arsenide phosphide (GaAsP), aluminum gallium indium phosphide (AlGaInP), or gallium (III) phosphide (GaP) (Craford 1992; Mukai 1999). Dopants producing blue light can be zinc selenide (ZnSe), or indium gallium nitride (InGaN) (Craford 1992; Mukai 1999; Xie 1992). LEDs can be used to produce light in a wide range of wavelengths, from 350 nm to 940 nm (Steigerwald et al., 2002), while having the superior control over the composition of the produced spectrum of light compared to all other commercially available light sources (Morrow,

2008). The efficiency of conversion of electric power to light depends on the input power. For the same peak wavelength, operating LEDs at higher power lowers their electric conversion efficiency compared to LEDs operating at lower power. Droop is defined as the electrical conversion efficiency loss as a function of operating power, and is affected by the polarizing fields that changes the dynamics of recombination of electrons and holes inside the junction (Kim et al., 2007).

The use of LEDs have been confined to low power, indicator lights in electronic devices (Figure 6) (Singh et al., 2015), but advances in technology have made LEDs a lot more powerful, compact, robust, durable, and efficient (Nelson et al., 2013; Morrow, 2008; Tsao et al., 2004). This expanded the potential fields of usage for LEDs and opened up entirely new areas of utilization. For example, LEDs now can be used in many high power lighting applications (Figure 7) (Singh et al., 2015) and are replacing incandescent lamps, fluorescent bulbs, and other high intensity discharge lamps as a source of electrical lighting in commercial greenhouses (Nelson et al., 2013; Tsao et al., 2004). It has been reported that LEDs can have an operation lifetime of up to 100K hours (Folta, 2005); however extreme temperatures and high operating currents will cause early degradation in output or life expectancy (Pecht et al., 2014; Van Driel and Fan, 2013). Increased PN junction temperature results in an exponential decline in the LED's lifetime (Fu et al. 2011). Even though some greenhouse conditions; such as high temperature and humidity can lower the longevity of the LEDs, they still retain a higher lifetime than that of current greenhouse lighting technologies (Fu et al. 2011).

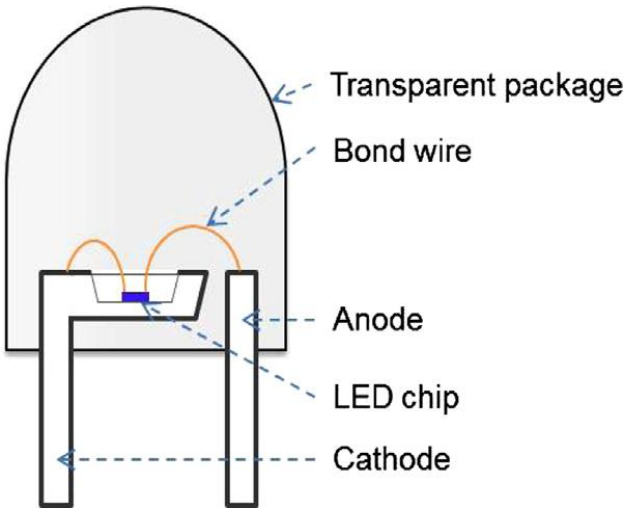

Figure 6: Key structure of a low wattage LED suitable as an indicator light source. It consists of a PN junction chip (light-emitting semiconductor), a lead frame containing the die, in addition to an encapsulation to protect the die (Singh et al., 2015)

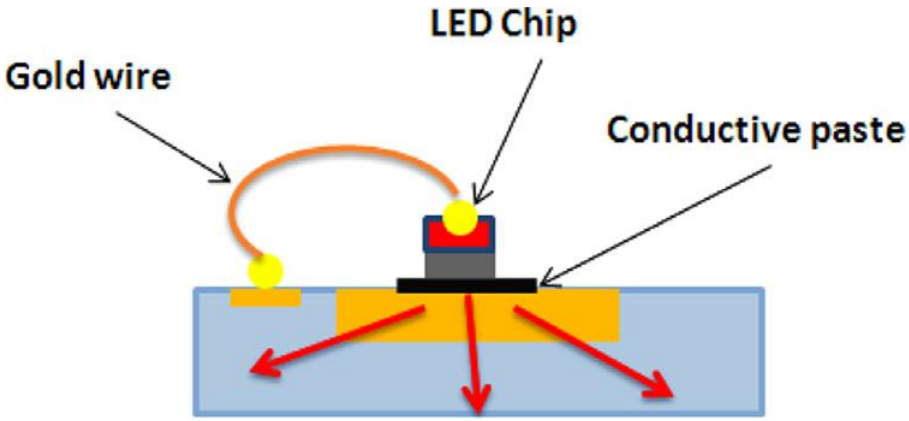

Figure 7: Chip on board or COB design of an LED which has an improved thermal conductivity, this design is the most commonly used one for high intensity LEDs, as it enables the dissipation of excess waste heat from the light emitting surface to an active heat sink, which in turn allows the light source to be placed close to the crop surfaces without risking to overheat or stress the plants (Singh et al., 2015)

1.4. LED usage for plant research

The unique properties of LEDs offer a number of benefits for researchers and growers. This includes an overall higher efficiency, resulting in a reduction in power consumption that can go up to 70% when compared to traditional lighting technologies (Singh et al., 2015). This is partly due to the unmatched capacity for spectral output optimization, and with advancement in LED technology, improving electrical conversion efficiency has played an important role, further lowering power consumption (Nelson et al., 2013; Tsao et al., 2010; Steigerwald et al., 2002). Different types of LEDs from the blue light region to the far-red region can be used in combination to tailor a specific spectral composition (Brown et al., 1995; Singh et al., 2015), maximizing spectral efficiency (Tamulaitis et al., 2005). This allows LEDs to be characterized by a high relative quantum efficiency (RQE), which means how efficient they are for photosynthesis (Singh et al., 2015; Martineau et al. 2012; Gómez et al. 2013) and enables researchers to experiment and study the effect of single or multiple wavelengths to determine what exact wavelengths are optimal for plant photosynthetic, photo-morphogenic, phototrophic and metabolic processes (Tamulaitis et al., 2005; Hyeon-Him et al., 2004). Conversely, HPS bulbs do not readily allow spectrum manipulation and optimization (Tamulaitis et al., 2005); additionally, both HPS and other HID lighting systems have a relatively limited spectral efficiency for plant growth (Bula et al., 1991; Morrow, 2008).

LED lights can be dimmed and brightened electronically in a simple manner, with the light intensity being linearly related to the input current and voltage within a voltage range that depends on the type of LED (Singh et al., 2015; King, 2008). A constant and optimal light irradiance can therefore be achieved, which can vary depending on the photosynthetic needs of the plant species being studied (Mathieu et al., 2004; Ieperen et al., 2008), LED lighting systems can be integrated into digital control circuits easily, which would allow automated control over their output and potentially counter temporal variation in solar irradiance (Tamulaitis et al., 2005; Tsao et al., 2010). This is a major advantage over gas discharge lamps, which operate under a fixed voltage and power with no direct control over output of light, or HID lights that

only allow for limited and indirect control, mostly done with shade control systems, which results in great energy losses (Mathieu et al., 2004). LEDs emit less heat in the direction of illumination compared to traditional light sources, this limits the risk of heat stressing plants when LEDs are used in close proximity to them, and enables the use of LEDs to maximize spatial uniformity of light and limit shaded areas, which helps in optimizing crop yields (Ieperen et al., 2008) and allows for better and more stable temperature control inside a growth chamber (Singh et al., 2015). This is another great advantage for LED lights compared to traditional lights like the typically high power HID, which cannot be placed closer than 1 meter to plant canopies due to heat stress and light saturation restrictions, which cause leaf burn and plant death (Dorais, 2003). Lighting systems utilizing LEDs have reduced cable gauge, which is translated to a reduced weight and low cabling costs (Singh et al., 2015). The above benefits, combined with the longer lifetime, increased durability and more compact size of LED light systems (Singh et al., 2015; Steigerwald et al., 2002), position LEDs as a technically advantageous choice for plant researchers and growers alike.

1.5. LED technical limitations

LED light sources produce reduced heat in the direction of light emission compared to traditional lighting sources (Singh et al., 2015). However, heat is still dissipated in the opposite direction of light emission, and increases as the input power to the LED is increased (Yung et al., 2013). In LEDs, heat generation is a result of non-radiative recombination of electrons and holes, which causes heat buildup in the junction (Gu and Narendran, 2004; Lee et al., 2001). The lower input power required by LEDs to operate means that dissipated heat is limited, but this excess heat lowers the photon conversion efficiency of the LED, shifts its peak wavelength, temporarily reduces its light intensity (Gu and Narendran, 2004; Schanda et al., 2014; Xi et al., 2005a; Yang and Cai, 2013) especially when junction temperature exceeds 100 °C (Christensen and Graham, 2009; Su et al., 2012) and eventually causes permanent degradation to the LED (Li et al., 2014; Xi et al., 2005b). The shift in peak wavelength due to excess heat can be from 10 nm to 15 nm towards longer wavelengths (Gu and Narendran, 2004; Peng et al., 1999) and the reduction in

light intensity is between 10% and 25% (Chang et al., 2012; Liu et al., 2009), with red LEDs suffering more from these effects than blue LEDs (Schanda et al. 2014). Heat buildup increases the possibility of non-radiative recombination, which further exacerbates these issues and results in more excess heat generation. Therefore, thermal management of LEDs is of crucial importance as it directly affects the reliability and efficiency of the light system, especially for research purposes, where any shifts in peak wavelengths or intensity are undesirable (Christensen and Graham, 2009). Thermal management can be adequately achieved using passive heat sinks, cooling fans, or water cooled heat sinks. Additional monitoring of the reliability and performance of LEDs is required for out-door operation to account for the variation of heat load caused by changes in solar radiation (McCartney and Lefsrud, 2018). For research applications, a programmed system is required to constantly monitor the temperature of the LEDs and actively control their cooling mechanism to minimize changes in the spectral properties of the LEDs due to heat.

Light uniformity is another aspect that should be considered when working with different light sources, whether it is the intensity decay from the source to the sample, or the horizontal intensity gradient at the surface of the sample (Nelson and Bugbee, 2014; Wallace and Both, 2016). Controlling light uniformity via secondary optics, such as reflectors and lenses, is critical for LEDs. The type of secondary optics needed depends on the application and the required beam angles, with low beam angle lenses providing light focus towards a targeted sample, and combining light from multiple LEDs, which improves the net photon utilization efficiency (Li et al., 2016; Poulet et al., 2014). Controlling the light intensity for LEDs can also be done by adjusting the distance between the light source and the sample while operating the source at the same input power, without the risk of heat-damage to the sample; this is an advantage for LEDs over traditional light sources (Both et al., 2017; Gómez et al., 2013; Massa et al., 2008). For chip on board LED sources with multiple LEDs of the same wavelength, lenses of beam angles from 60 to 120 degrees are typically used, with lens design and LED diode arrangement on the chip tuned to circumvent intensity heterogeneity caused by constructive and destructive

interference of light emitted by the group of LEDs forming the luminaire (Chen et al., 2011; Whang et al., 2009).

1.6. Stepper Motors

Stepper motors are a type of brushless DC motors that provide controlled motion and precision positioning. Stepper motors divide the rotation cycle into a number of equal sized steps (Tarun, 2013). A stepper motor requires a controller to function, and typically features an open-loop setup, where the operation sequence is predetermined and remains the same within an allowed load limit (Tarun, 2013). In simple terms, a unipolar stepper motor consists of a rotating gear at the center of the motor, surrounded by a series of electromagnets. The central gear is connected to the motor shaft. The electromagnets are energized and deactivated in series, with each activated electromagnet attracting and aligning the teeth of the gear to it, and placing them in slight offset relative to the next deactivated electromagnet. When the next electromagnet activates, it corrects this offset and aligns the teeth of the gear to it, resulting in a stepped motion. This process is repeated in series for all the electromagnets present within the motor. Once a full activation cycle is done, the stepper motor would have rotated the equivalent of a single tooth position (Tarun, 2013). In reality, the electromagnets are not activated one at a time, but are rather divided to groups called phases, each group is activated at the same time, and the electromagnets of each group are always separated by those of other groups, in an alternating pattern. A disassembled stepper motor is shown in Figure 8 (retrieved from https://emadrlc.blogspot.com/2013/01/stepper-motor-construction.html).

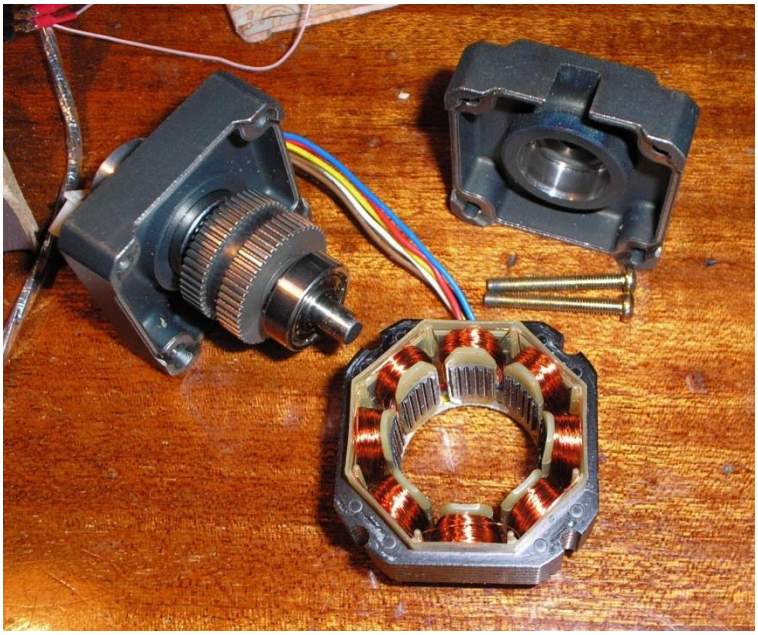

Figure 8: A disassembled stepper motor

1.7. Cuvette Systems

Cuvette systems utilize light sources, small containers carrying a test sample and spectrophotometers to study the interactions between specific wavelengths of light and the sample; which is dissolved in a solvent or suspended in a fluid within the cuvette, in a technique known as optical absorption spectroscopy (Merzlyak et al. 2008). Optical absorption spectroscopy is applied in the study of biological and chemical substances including photosynthetic pigments (Merzlyak et al. 2008). The shape of the cuvette container varies to accommodate different testing requirements, and the sample may be static in the container (Hervey et al. 2021) or may be dynamically flowing through the cuvette, which in this case must utilize multiple ports to support sample flow (Evans et al. 2022).

Light scattering by the test sample can affect the apparent absorbance at individual wavelengths (Merzlyak et al. 2008), this can cause complex distortion in absorption measurements that varies according to the wavelength of light and the structures present in the sample (Merzlyak et al. 2008). The optimal method of dealing with scattering is through the use of an integrating sphere, which is built in high-end spectrophotometer to collect the scattered light at the detector (Merzlyak and Naqvi 2000). However, research using simpler

spectrophotometers have devised different, less costly techniques to limit the effect of scattering, mostly through the use of various diffusers at the light incidence surface of the cuvette to uniformly scatter incoming light beams, rendering sample scattering negligible compared to diffuser induced scattering in the final observed spectral recordings (Jackson et al. 2014). Hervey et al. proposed a diffusion technique that utilizes a dual compartment cuvette, the first compartment facing the light source is filled with a suspension of titanium dioxide in water, and the other compartment facing the sensor carries the sample (Hervey et al. 2021). Titanium dioxide, which is inexpensive and easily available, forms an opaque suspension in water allowing the solution to act as a diffuser (Hervey et al. 2021). This technique has resulted in reproducible spectral readings when tests are repeated using the same particle size and concentration of titanium dioxide, and allows for an inexpensive and standardized diffusion stage compared to other diffusion techniques (Hervey et al. 2021).

Most applications utilizes cuvettes made of clear, transparent material to analyze the light beams that passes through the sample when it emerges from the other side of the cuvette (Merzlyak et al. 2008, Merzlyak and Naqvi 2000, Hervey et al. 2021). However, some applications utilize cuvette systems that have cuvette containers made of reflective metal, and use the reflected or scattered beams bouncing off the metal of the cuvette as an input to spectral analysis setups (Lykina et al. 2017). A concentration of albumin, the most common protein in blood plasma, was tested with a Raman spectroscopy setup where the pumping efficiency of the laser light source was increased by allowing more multi-reflections to occur within custom made, aluminum cuvettes of various volumes and shapes (Lykina et al. 2017). It was found that cuvette-reflectors with a smaller volume and a spherical bottom resulted in a twofold increase in the accuracy of the registration efficiency of the albumin Raman signals, allowing for a reliable and efficient method of detecting abnormality in albumin concentration, which is indicative of organ pathology or body inflammation (Lykina et al. 2017).

2. Chapter 2: Designing the Cuvette System

2.1. Initial Pigment tests

The Biomass Production Laboratory performs studies focused on plant pigments and their properties, these tests involve the spectral analysis of solutions of the photosynthetic pigments in various solvents, and observing the absorption characteristics of these pigments. This plays an essential role in the bigger purpose of understanding and researching photosynthesis, and can pave the way to the advancement of technologies and sciences that can harness the mechanisms of photosynthesis to serve a broad range of applications, benefiting the environment as well as humanity.

At the start of this project, a number of these light analysis tests were performed, specifically using solutions of chl a in acetone, chl a in canola oil, chl b in acetone and chl b in canola oil. The tests were performed by mixing the chlorophyll samples; which are in powder form, in solvents like acetone or canola oil at different concentrations and analyzing them using a spectrophotometer to determine their absorbance profile in the action spectrum region of light. The baseline test will not be included in this thesis, as they in themselves are out of the current scope.

The tests were performed by preparing the samples in test tubes, adjusting the concentrations of the solutions, and placing them in small glass cuvettes designed to work with the spectrophotometer, then performing a light scan with the samples multiple times and recording the absorbance profile. The tests samples were mixed, prepared and transported to the spectrophotometer under low lighting conditions, to avoid any damage from sunlight or room lighting. The only significant light the samples were subjected to is the light of the testing station. The spectrophotometer used was an Ultrospec 1100 pro UV/Visible spectrophotometer; this model performs spectral analysis on a sample placed in a small, open-

top glass cuvette, and shines the testing light horizontally inside the testing compartment of the device.

2.2. Reasoning behind the Cuvette System and its Main Requirements

The new cuvette testing platform was built to compensate for the limitations of the existing spectrophotometer. The existing device; as stated above, shines light from a fixed horizontal angle through the sample in a small, open-top glass cuvette, placed in a compartment within the device. This immediately creates a few limitations.

The fixed, horizontal angle of light incidence makes it impossible to test samples of heterogeneous nature. For example, a certain pigment dissolved in water and another pigment, or the same one dissolved in oil. There is a need to study light behavior on such type of samples and how the water-oil interface affect incident light at different angles to the interface plane where water meets oil. The existing system would not be able to test these samples, since it shines light horizontally, parallel to the interface plane.

The small size of glass cuvette in the existing system would make it very challenging to prepare a larger sample of multiple solvents. The fact that it is also open-top would make it impossible to monitor any pressure buildup in the sample as a result of light incidence, and would subject the sample to atmospheric air, possibly for extended time, causing potential contamination to it. Since the glass cuvette is placed in an enclosure inside the existing spectrophotometer, the possibility of adding any other external sensors to monitor changes in the temperature of the sample, or reflectance via additional light sensors is nullified. The LED light source and light sensor inside the existing system are built-in, and no exchangeability is supported.

The new cuvette system is not intended to fully replace the existing spectrophotometer, but is meant to be a platform for a more flexible testing device that extends and enhances the amount and type of data that can be observed and gathered from the samples as they are subjected to light. The new cuvette system needs to shine light vertically, and different angles,

to allow the testing of heterogeneous samples. The angle of incidence of the light must be variable and easy to adjust on the go. The glass cuvette used must be sealed and of a slightly larger size to simplify the testing of complex samples, and the addition of extra sensors in the future. The LED light source, light sensor, and glass cuvette must be swappable with other different sources, sensors and cuvettes, respectively. So the new system needs to be modular, and support interchanging these parts with no adjustments in the frame, or with limited adjustments if necessary. And the new system must be designed to work with LED light sources and light sensors currently available in the Biomass Production Lab, to minimize the budget of the system, while offering the potential for the use of other light sources in the future. Using these existing LEDs, a minimum light intensity of 250 µmol m^{-2} sec^{-1} at the center of the glass cuvette surface is required, regardless of the LED used. These are considered the main requirement of the new cuvette testing platform.

2.3. Description of the proposed design

The cuvette system's frame is composed of 3 steel plates, one being the base and two represent the sides. Steel was chosen for the frame to limit any vibrations during the tests, and to allow for a higher lifetime for the device overall. The base plate is 0.5" in thickness, 12"in length and 9"in width. The two side panels have a thickness of 0.5", width of 12" and Length of 14". These plate dimensions are; to an extent, limited by what the steel supplier avails, but are suitable for the build and allow some extra room for the addition of external sensors at a later time. The base panel holds the two side panels, at both ends of it, with a separation of 9", facing each other and orthogonal to the surface of the base. The right side panel has an outer L-shaped shelf to hold the stepper motor. It has a port for the shaft of the motor to go through; the shaft would carry a rotating arm, which would be centered opposite to the glass cuvettes. The opposite, left side panel holds a stationary, horizontal steel arm, at the end of the arm is an exchangeable adaptor that holds the glass cuvette without touching it through the use of rubber rings, the adaptor does not interrupt the line of sight between the light source and the sensor. During the design phase, the need for a mixing mechanism to be implemented on this

side of the device was examined, but after the preparation and testing of chl a and chl b pigments in canola oil and acetone, the mixer mechanism was excluded from the final design. This is due to the observed ease of solubility, and lack of precipitation of these pigments in the tested solvents. This side of the device is static as a result, and serves as a holder to glass cuvettes. The dimensions of the two side panels and the base were selected to accommodate the rotating arm, and then were fine tuned to match the provided steel plate dimensions offered by the steel supplier, in order to minimize the required budget and effort needed to shape the plates. Also, no welding along the length of the individual plates was done to maximize the overall build integrity and avoid irregularities in the frame.

The right side panel hold the stepper motor, attached to its shaft is a rotating arm made of steel; this material was selected for its longevity, and to allow for a secure mounting of the light source and a light sensor. The rotating arm has a horizontal axis of rotation; along this axis are the glass cuvettes, which are aligned so that the center of its surface would be exactly below the light source above and also directly above the light sensor at the lower end of the rotating arm. The rotating arm length was determined by testing the light sources that will be used in the device. A minimum light intensity threshold of 250 µmol m^{-2} sec^{-1} at the center of the glass cuvette surface was required, so LEDs of different wave lengths were tested to determine the maximum distance from the LED to the surface of the sample that would satisfy this requirement. Using a UV LED (410 nm) which by design had the lowest output power, a spacing of 10 cm from the edge of the LED to the glass cuvette was determined. At this distance, the amber light LED (595 nm) which is of particular interest to our research group, would produce an intensity of 450 µmol m^{-2} sec^{-1} at the surface of the glass cuvette. The length of the arm accounts for the size of the glass sample chamber; which is at the center of the rotating arm's prongs, and the thickness of the LED light source and its water-cooling jacket. As a result of the above, the final lengths of the rotating arm was determined to be 25 cm, this includes the spacing between the light source at the higher end of the arm and the glass cuvette, the height of the glass cuvette and the spacing between the lower surface of the glass cuvette and the light sensor at the lower end of the arm. The rotating arm is attached to the motor at the

middle of its length, at the upper end, it has a mount for the metal water-cooling jacket of the LEDs used in the tests, the cooling system is necessary for the LED to operate at the desired wavelength, it needs a constant supply of water, so the cooling jacket has and input port for cool water and an output port for hot water, water is delivered and extracted from the cooling jacket using two rubber water tubes, each of a diameter of 1 cm. On the opposite end of the rotating arm, a light sensor is mounted along the same axis as the light source and center of the glass cuvettes.

To provide rotational motion for the rotating arm over a horizontal axis, a stepper motor was used. Stepper motors are a type of brushless DC motors that provide controlled motion and precision positioning. Traditional “brushed” DC motors use two or more stationary contact brushes -typically made from graphite- to deliver electric current to the windings of the rotor, by pressing against the commutator. This has a number of disadvantages, power loss from the friction between the brushes and commutator, the wearing down of the brush material which can create a fine dust and possibly interfere with the sample, and the abrupt repeated current switching in the rotor’s coil –which has an inductance- creates sparks at the commutator and brushes point of contact, these sparks create electronic noise, which can interfere with the sensors and possibly the sample. Brushless DC motors do not use the commutator and brushes setup, and rely instead on an electronic servo system, where –generally- the angle of the rotor is electronically detected and the current in the windings is controlled to maintain a unidirectional torque. This gives the brushless motor increased efficiency, longer lifetime, and less electronic noise. Another key advantage for our design is that brushless motors rely on electronics for commutation, this allows for greater flexibility with regards to controlling the rotation of the motor, like speed limiting and micro-step operation for precision positioning. These capabilities are not available using traditional DC motors.

3. Design Implementation

3.1. Additional Design Requirements

For this cuvette system design, it is required to:

- Rotate an arm carrying a light source at one end and a light sensor at the opposite end, around a fixed glass cuvette containing a sample.
- The rotation must be controlled, slow, and reversible. The wiring to the light source and light sensor and the water cooling tubes that are fixed along the arm could be damaged by uncontrolled or abrupt motion.
- The experiments that need to be performed by the device require a defined set of angles of incidence relative to the sample.
- The sample must be kept in the cleanest conditions possible, even though it is in a sealed glass cuvette, any dust particles can obstruct the path of light from the source to the sensor.
- The glass cuvette has a light sensor close to it, and therefore sources of electronic interference can affect the reading of the sensor.

These conditions led to the decision of using a stepper motor in this build.

3.2. Building the Cuvette System

Four plates, two of them had the dimensions of the side plates, and another two with the dimensions of the base plate were selected (Lachine Steel, Lachine, QC). Additional steel rods required for the arm and the cuvette and motor support were obtained from the workshop storage. The stepper motor used was a ZABER X-NMS Series stepper motor, it comes with a built in modulator and controller in addition to its own power supply. This model is equipped with a built in knob that can be turned to manually adjust the angle of the shaft, and by extension the arm.

Two glass cuvettes were purchased for this build; the first is an Alpha Nanotech quartz cuvette with a screw cap and septum, and the dimensions of 12.5 mm x 12.5 mm x 58 mm, with a 10 mm light path. The second cylindrical one from FireflySci is larger, made of optical glass with two stoppers, with a length of 52.5mm, diameter of 22.0mm, and a light path of 50 mm. The first, rectangular cuvette is intended for use with single solvent samples, while the second cylindrical one would be more suited for multi solvent samples due to its larger capacity. The material for both cuvettes has uniform transmittance across the wavelength spectrum of interest. There is one sensor so far in this build, a spectroradiometer (PS-300, Apogee, Logan, UT). As for the LED light source, it can be interchanged as long as it is fixed to a heat sink with the same dimensions as the one the design was based on, specifically a CN40-15B 40 mm Round x 15 mm High Alpha Heat Sink - 10.7 °C/W. However, the LED that was attached and tested for the final build was a SP-02-W4 Cool White (6500K) Rebel LED on a SinkPAD-II 40mm Round 7-Up Base - 840 lm, and was fitted with a 263 Polymer Optics 7 LED Cell Cluster Concentrator Optic lens.

The cuvette system was built in the workshop on the Macdonald Campus of McGill University. It started with drilling eight unthreaded holes in the base plate, two in each of the four corners, to fit eight ¼ inch bolts, these holes were also flushed from the lower side of the base to allow it to fully rest on a surface once the bolts were placed. The extra steel plate; with the exact dimensions as the base, was used to provide steel pieces for the diagonal support of the frame, this was done by sawing off the four corners of this plate using a belt saw. These four triangular diagonal support pieces were drilled two times each at the base plate facing side into the thickness of each triangular piece; these holes were also threaded to accommodate the tightening of two ¼ inch bolts each, allowing the base to be attached to the diagonal support pieces. The left and right steel plates were also drilled four times each and the unthreaded drill holes flushed for four ¼ bolts each. Once this was done, the four diagonal support pieces where bolted to the base plate, the side plates were placed in location and four temporary welds were done to attach the side plates to the diagonal support. The diagonal support pieces; with the side plates temporarily welded to them, were unbolted from the base plate, and taken to the

table drill, where two additional holes were drilled through the existing holes in the side plate into each welded diagonal support piece. Once this was done, the temporary welds were removed and the plates where grinded from any remaining welding metal. The two new holes in each diagonal support piece were then threaded as well. The diagonal support pieces therefore; keep the three frame plates attached to each other. The main frame is shown in Figure 9.

The right side plate was then disassembled from the rest of the frame, and a plasma cutter was used to open a port for the shaft-side of the stepper motor, this port was then evened and made into a square shape with a milling machine, excess steel was then cleaned off the plate with a grinder. An L-shaped tray to hold the motor was then formed from a steel rod, and drill holes in the tray and the right side plate were done to fix the tray directly below the shaft port with ¼ inch bolts and nuts. Holes were also drilled in the tray itself so the bracket of the motor can be screwed to it. A steel rod was selected to form the rotating arm, square pieces of this rod were cut and welded to sides of the rod at each end, and these ends will be holding the LED light source and the base of the light sensor. Figure 10 shows the results so far.

The straight steel rod was then orthogonally bent at each end to form the final shape of the arm, with the two prongs of the rod facing one another. Holes were drilled through the center of the arm to accommodate the shaft of the motor, and the attachment of the wheel hub that keeps the shaft of the motor fixed to the arm. At the ends of the arm, holes were drilled to attach the heat sink of the LED light source to the arm at the top, and the base of the light sensor at the opposite end of the arm; the results so far are shown in Figure 11 and 12.

The left side plate of the frame was drilled and attached to another orthogonally bent steel rod via nuts and bolts; this rod will be holding the cuvette glass to the left plate. The end of the holder was drilled to attach two different and interchangeable metal adaptors, one for each

glass cuvette. These two adaptors were made from steel rods that were bent, drilled and smoothed. And each was designed specifically for the corresponding type of glass cuvette. The adaptors do not make actual contact with the glass of the cuvettes, as this might cause damage and scratching to the glass, so rubber rings are placed between the glass cuvettes and the surface of the steel adaptors. Figure 13 and Figure 14 show the assembled system with both types of glass cuvettes separately equipped.

Figure 9: The assembled main frame of the cuvette system

Figure 10: The motor port and holding tray

Figure 11: The rotating arm attached to the motor with a dummy heat sink and the actual light sensor

Figure 12: Outside view of the above, showing the stepper motor on its tray

Figure 13: Assembled cuvette system with the cylindrical glass cuvette equipped

Figure 14: Assembled cuvette system with the rectangular glass cuvette equipped

Once work on the build was completed, it was disassembled. Each part of the main frame was branded with numbers and letters to indicate its correct position and order of assembly for future users, all steel parts were spray painted with anti-rust flat black paint, to offer some protection, and limit the effect of light reflection off the steel parts when performing tests. It is worth noting that the entire build was done precisely in one go, without any mistakes or repetitions. The paint was given a day to dry, then the system was transported to the Biomass Production Lab for testing. Figure 15 to Figure 20 show the final assembled system from multiple angles.

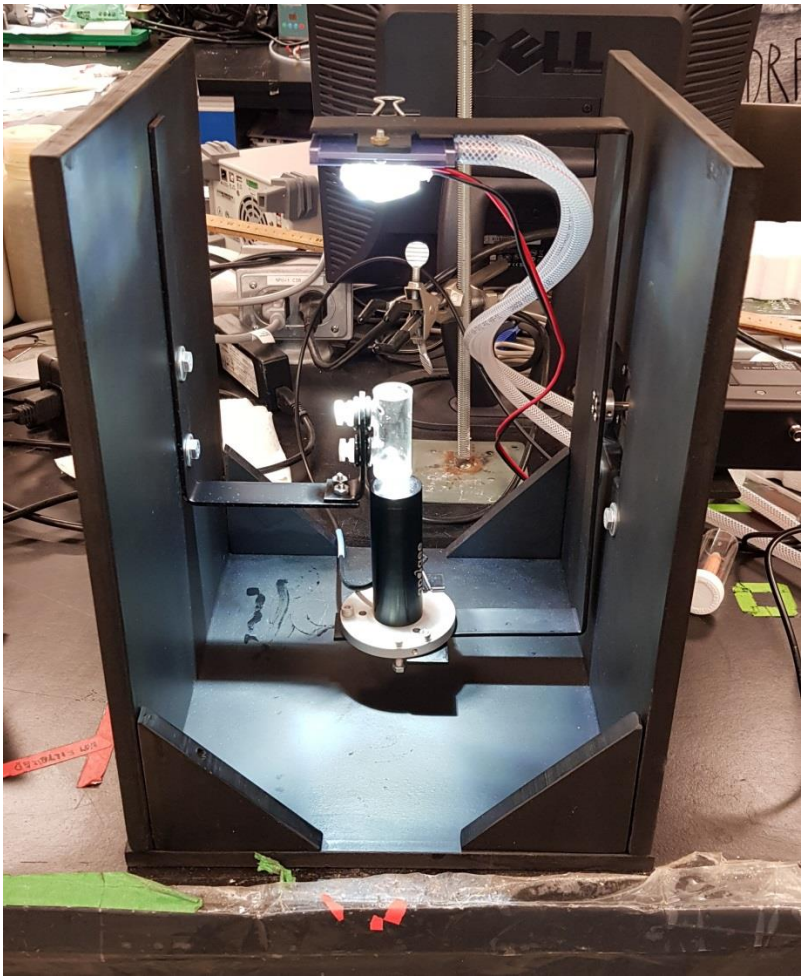

Figure 15: Front view of the system. The two side panels have a thickness of 0.5”, width of 12” and Length of 14”. The rotating arm has a length of 25 cm

Figure 16: Side view of the system, showing the panel holding the glass cuvette

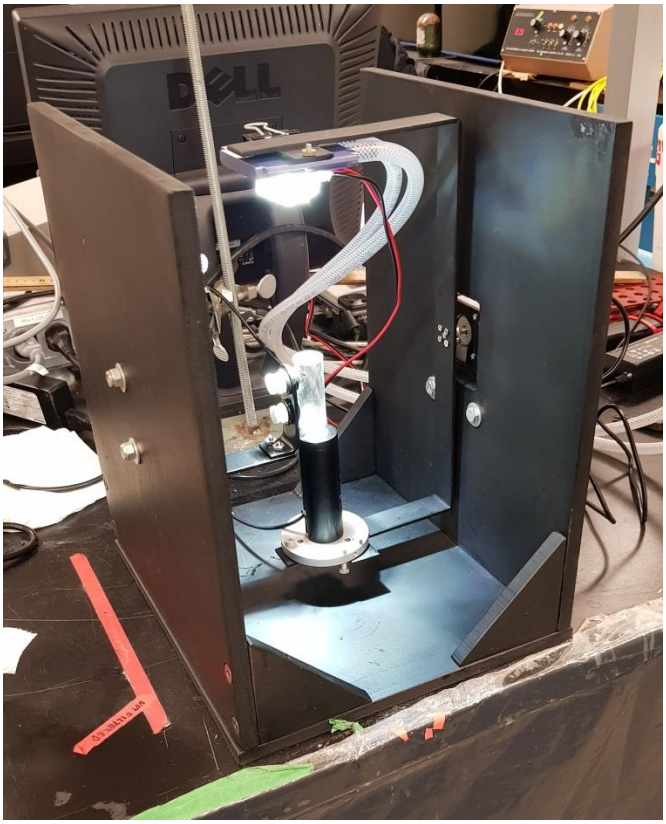

Figure 17: Diagonal view of the system

Figure 18: Diagonal view of the system

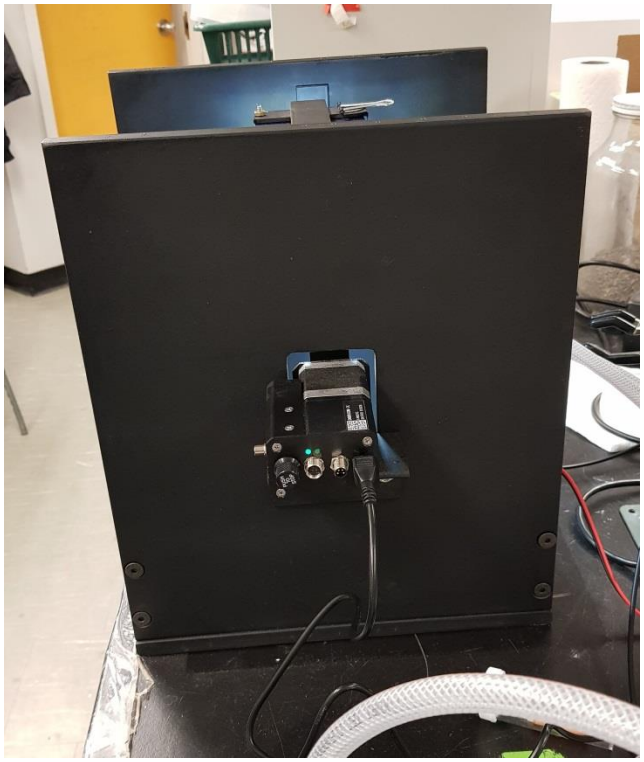

Figure 19: Side view of the system, showing the panel housing the stepper motor

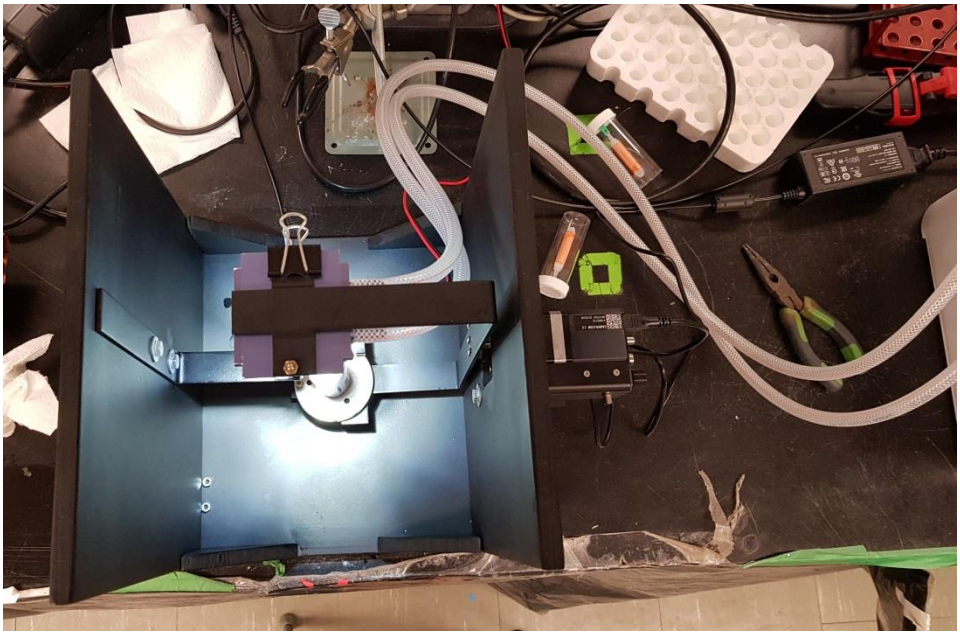

Figure 20: Top view of the system. The base plate is 0.5” in thickness, 12”in length and 9”in width [side plate to side plate].

4. Final Result and Tests

Once the Cuvette system was transported to the lab, it was assembled and two benchmarking tests were performed. The LED light source was connected to a DC power supply (DP832, Rigol Tech., Beaverton, OR, USA), the stepper motor was connected to its own DC power supply, and the water-cooling heat sink was connected to an iso-temp bath circulator (4100R20, Fisher Scientific, Hampton, NH, USA) that circulated water at a temperature of 15 °C.

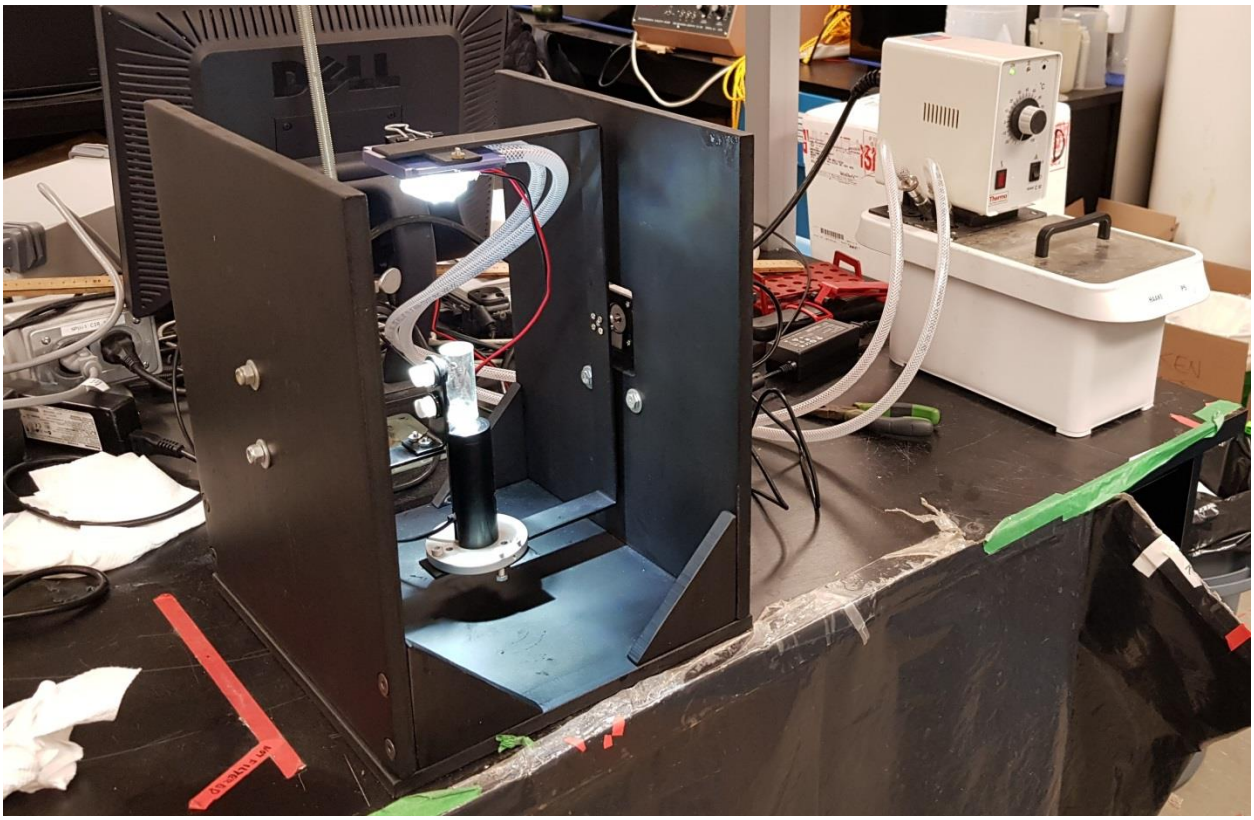

Figure 21: The entire testing setup, showing the assembled cuvette system and iso-temp bath circulator

Twenty-four benchmark tests were done using the cylindrical and rectangular glass cuvettes, the samples were blank samples of water and mineral oil at vertical (0°) and horizontal (90°) light incidence to the sample surface. Additionally, four other incidence angles were tested by rotating the arms of the system by one to four steps, with each step incrementing the angle by

3° 45'. The reason for the small step angle is to ensure that the light source, top surface of the glass cuvette, bottom surface of the glass cuvette and the spectroradiometer all lie along a straight line at the fourth or maximum step, for both cuvettes. And for a clear comparison, these angles were kept the same for both glass cuvettes, even though the cylindrical cuvette was the determining factor in the selection of the angles, since it has a larger depth. The below figures demonstrate the transmittance results obtained from the tests. The vertical axis denotes the relative spectral transmittance, while the horizontal axis denotes the wavelength in nm. It is worth noting that the cylindrical cuvette exhibits a significant lensing effect compared to the rectangular cuvette, especially with an oil sample.

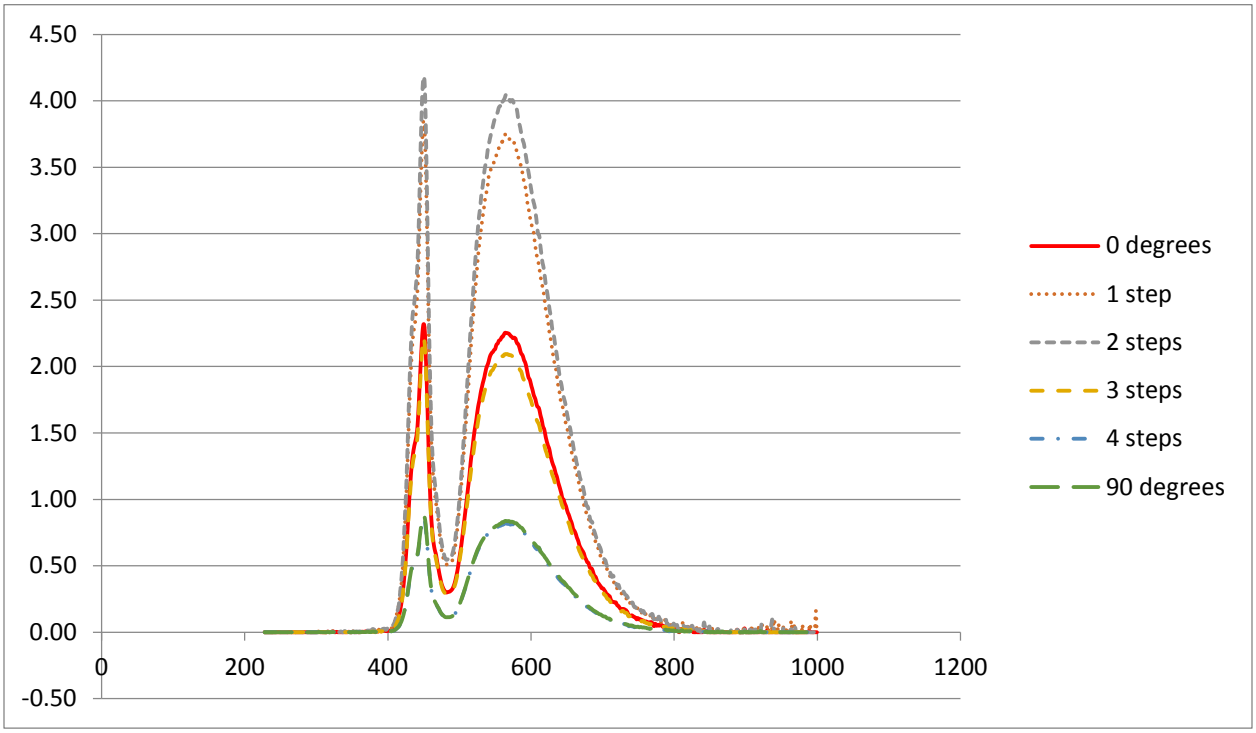

Figure 22: Cylindrical cuvette with mineral oil comparison, a step is 3° 45'

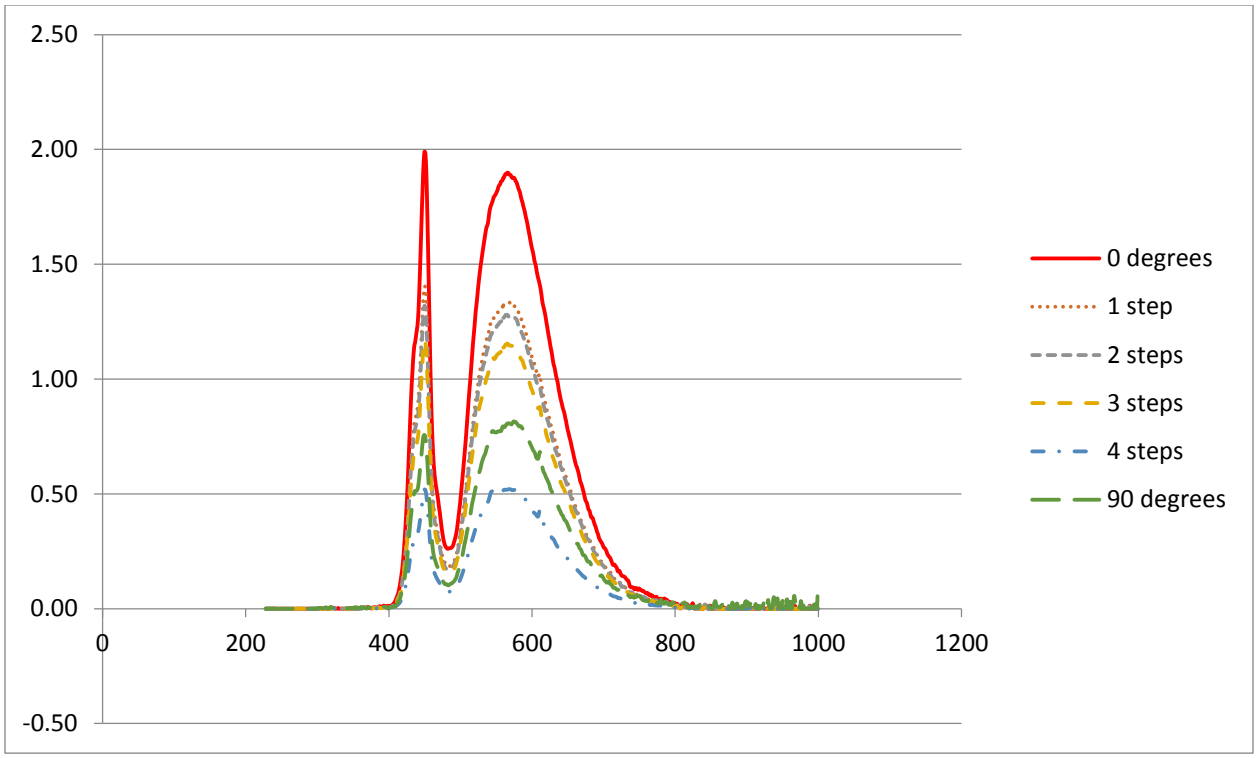

Figure 23: Cylindrical cuvette with water comparison, a step is 3° 45'

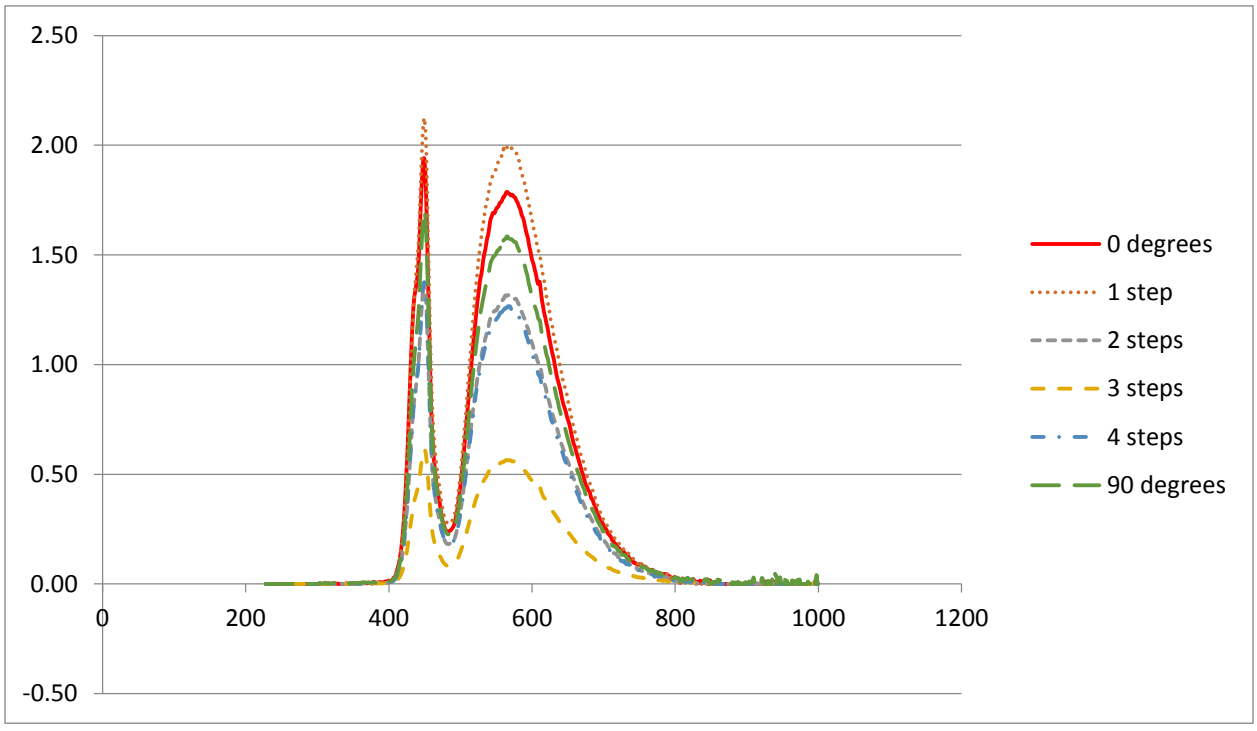

Figure 24: Rectangular cuvette with mineral oil comparison, a step is 3° 45'

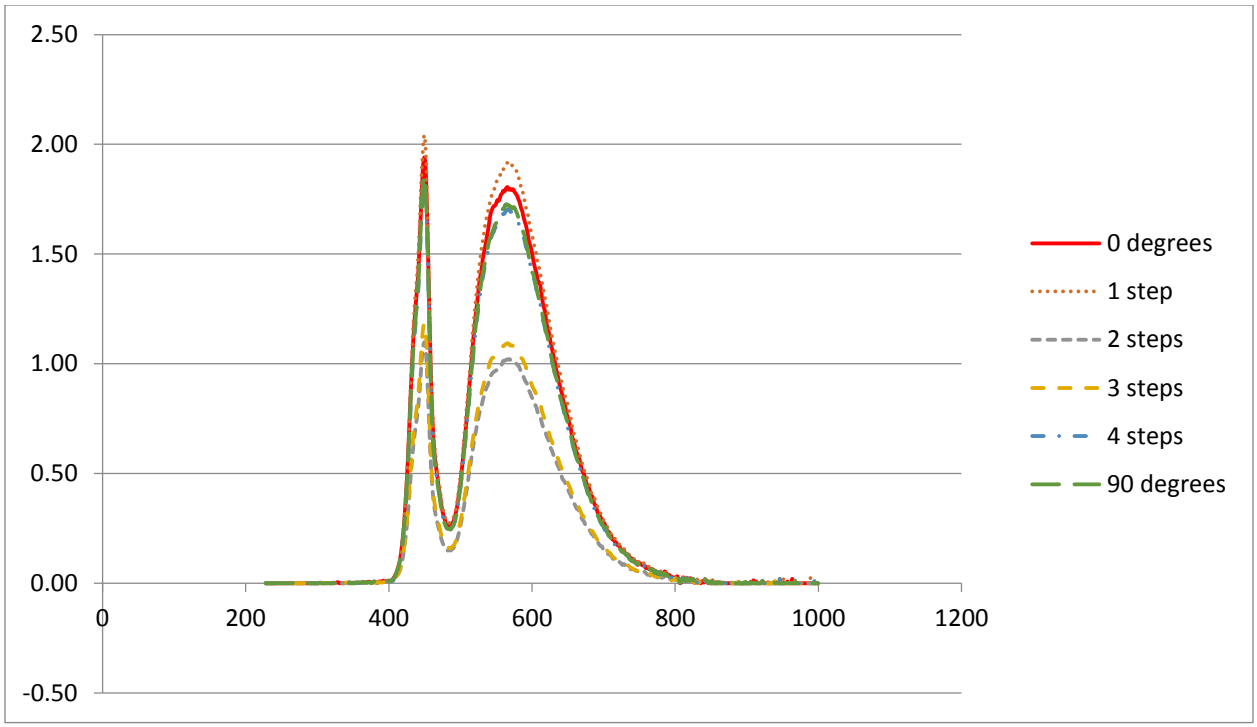

Figure 25: Rectangular cuvette with water comparison, a step is 3° 45'

The test results show that the lensing effect varies between the 2 cuvette shapes, the sample type used, and the angle of incidence. A sample in mineral oil results in the highest amplification of intensity by both cuvette shapes, with that effect being strongest with the cylindrical cuvette (significant in step 1 and 2) than with the rectangular cuvette (step 1). As for water samples, the cylindrical cuvette results in a decline in intensity as the angle of incidence is increased, while the rectangular cuvette exhibits an increase in intensity at step 1, then a decline at the following steps. This effect occurs due to the constructive and destructive interference of multiple pathways of incident light, which is affected by the refractive index of the sample solvent used and the cuvette material itself. It is worth noting that the tests are only for benchmarking, and that the above results only show these effects at the predetermined test angles, and that there may be more peaks and troughs in intensity in between the angles tested.

It is important to account for lensing by performing blank solvent tests at the desired angles before adding actual samples and running the tests at the same angles.

LED light passes through multiple media interfaces on its way to the spectroradiometer, from air to glass at the top of the cuvette, from glass to the liquid within the cuvette, it then travels through the sample and reaches the bottom of the cuvette, where it passes through the interface between the liquid and the glass bottom, and the glass bottom and air interface to reach the light sensor. At each of those interfaces, a ray of light will experience refraction, reflection or total internal reflection depending on the initial medium material, the target medium material and the angle of incidence at the interface plane (Dill et al., 1977). Total internal reflection can occur when light traveling within an initial medium where its speed is low compared to its speed in the target medium at the interface between both media, if the angle of incidence is larger than a certain critical angle (Jenkins et al., 1976). This effect happens within the walls of the glass cuvette as the light travels through the sample and interacts with the side of the glass cuvette, or through the top of the side walls directly from the LED source. The above effects increase the potential for multipath propagation of light waves, and those waves interact with one another causing constructive and destructive interferences at the light sensor, which leads to lensing or dimming effects at the spectroradiometer.

The light interactions within the glass cuvettes may be likened to light interaction in an optical fiber. In fiber optics, light is kept confined inside the fiber core, and prevented from exiting through the sides, by building the core with a material of a slightly higher refractive index than the cladding surrounding the core (Gloge, 1971). This keeps light propagating inside the core of the fiber by undergoing continuous total internal reflections, so long as light is guided into the fiber at an angle that does not exceed its acceptance angle, which is measured outside the fiber to ensure that a sequence of total internal reflections take place at the core-cladding interface once light rays are guided into the core (Hecht, 1999). The key difference between fiber optics and glass cuvettes is that in a glass cuvette, the refractive index of the solvent; whether it is

water or mineral oil, is lower than that of the surrounding glass (Zajac, 2003). However, there are similarities between propagation of light within the side walls of the glass cuvette, and light propagation along the core of an optical fiber. The side wall of a glass cuvette has an interface with air, and another with the solvent, with both of them having a lower index of refraction than the glass material of the cuvette (Zajac, 2003), therefore as light is shone at the top of the cuvette, it travels through the walls, undergoing a series of total internal reflections till it emerges from the bottom of the cuvette, similar to light propagation in the core of a fiber. It is worth noting that there are many differences between the two cases, the difference in shape, material, light path, and dimensions between an optical fiber and a glass cuvette are obvious, in addition to the manner of light source and receiver coupling, which is of great importance for effective information transmission in fiber optics (Goff, 1999), versus shining light from the LED source in the tested design and recording transmittance at the spectroradiometer, while both are separated from the glass cuvette itself.

5. Recommended Future Features and Improvements

The final cuvette testing system is intended to be a modular platform for the spectral analysis of pigment solutions. Therefore, there is a great room for improvement and additions. More testing with the new system in its current state is recommended, using different pigments and solutions at various concentrations, and comparing the obtained results to the results from the existing spectrophotometer. Additional light sensors can be placed inside the system to examine reflectance to the sides of the glass cuvettes. A form of light cover can be implemented to provide dark conditions in the vicinity of the light beam. A redesigned rotating arm with adjustable length can be implemented. Coding predefined angles to the stepper motor controller to quicken testing preparation is possible. The most complex improvement to the system is the addition of pressure sensors to the glass cuvettes to monitor pressure build up, this may require the replacement of the current cuvettes with custom made ones that can support the usage of a pressure sensor, something that will require some modification in the steel holder for the glass cuvette.

6. Summary

This thesis has examined the need for a modular cuvette system for light analysis of pigments; the requirements of such system were gathered by conducting preliminary tests using the current available spectrophotometer system. A proposed design was implemented; using a newly built steel frame in addition to readily available parts, in the workshop on Macdonald Campus. The final cuvette system was used to perform twenty-four benchmarking tests, after being transported to the lab. More tests are recommended with the new system, and additional features could be implemented to expand the flexibility of the system, and provide more types of data about the samples being tested.

References

Cooper, GM. 2000. The Cell: a molecular approach, 2nd edition. Sinauer Associates, Sunderland Mass.

Mishra, S. 2004. Photosynthesis in Plants. Discovery Publishing House, New Delhi. P. 1-165.

Farabee, MJ. 2007. On Line Biology Book, Photosynthesis. Estrella Mountain Community College, Azondale, AZ.

Lockstein, H., B. Grimm. 2007. Chlorophyll Binding Proteins. Encyclopedia of Life Cycles. John Wiley & Sons, New York, NY.

Sandmann, G 2001. Carotenoid biosynthesis and biotechnological application. Arch. Biochem. Biophys. 385:4-12.

Frank, HA, RJ Cogdell. 1996. Carotenoids in photosynthesis. Photochem. Photobiol. 63:257-264.

Demmig-Adams, B, AM Gilmore, WW Adams, III. 1996. In vivo functions of carotenoids in higher plants. FASEB J. 10:403-412.

Singh, D., C. Basu, M. Meinhardt-Wollweber, and B. Roth. 2015. LEDs for energy efficient greenhouse lighting. Renewable and Sustainable Energy Reviews 49:139-147.

Wozniak, B., J. Dera. 2007. Light Absorption in Sea Water. Springer Science and Business Media.

Heber U, VA Shuvalov. 2005. Photochemical reactions of chlorophyll in dehydrated photosystem II: two chlorophyll forms (680 and 700 nm). Photosynth. Res. 84:85-91.

Hopkins, WG, NPA Huner. 2004. Introduction to Plant Physiology, 3rd ed. John Wiley and Sons, Hoboken, NJ.

Köst, HP. 1988. CRC handbook of chromatography plant pigments. CRC Press, Inc.

Taiz L, E Zeiger. 1998. Plant Physiology, 2nd ed. Sinauer Associates, Inc. Sunderland, Mass.

McCree, KJ. 1971. Significance of enhancement for calculations based on the action spectrum for photosynthesis. Plant Phys. 49:704-706.

McCree, KJ. 1972a. The action spectrum, absorption and quantum yield of photosynthesis in crop plants. Agric. Meteorol. 9:191-216.

McCree, KJ. 1972b. Test of Current Definitions of Photosynthetically Active Radiation against Leaf Photosynthesis Data. Agric. Meteorol. 10:443-453.

Gagne, J.D., M. Lefsrud., M. Schwalb. 2012. Leaf Spectral Response Profiles in Tomato (Solanum lycopersicum), Petunia (Petunia hybrida) and Lettuce (Lactuva sativa) Plants Grown Under Sun VS. Fluorescent Light. Unpublished Manuscript. Department of Bioresource Engineering, Mcgill University, Montreal, Canada.

Gruszecki, WI, W Grudzinski, M Matula, A Banaszek-Glos, P Kernen, Z Krupa, J Sielewiesiuk. 1999. Xanthophyll pigments in light-harvesting complex II in monomolecular layers: localisation, energy transfer and orientation. Biochimica et Biophysica Acta 1412:173-183.

Koning, RE. 1994. Light. Plant Physiology Information Website. http://plantphys.info/plant_physiology/light.shtml.

Young, AJ. 1991. The photoprotective role of carotenoids in higher plants. Physiologia Plantarum 83: 702-708.

Müller, P, L Xiao-Ping, KK Niyogi. 2001. Non-Photochemical Quenching. A Response to Excess Light Energy. Plant Physiol. 125:1558-1566.

Demmig-Adams, B, AM Gilmore, WW Adams, III. 1996. In vivo functions of carotenoids in higher plants. FASEB J. 10:403-412.

Demmig-Adams, B. and Adams, W.W. III, 1992. Photoprotection and other responses of plants to high light stress. Annu. Rev. Plant Physiol. Plant Mol. Biol. 43:599-626.

Mozzo, M., L Dall'Osto, H Hienerwadel, R Bassi, R Croce. 2008. Photoprotection in the antenna complexes of photosystem II : role of individual xanthophylls in chlorophyll triplet quenching. J. Biol. Chem. 283(10): 6184–6192.

Barreiro, R, JJ Guiamet, J Beltrano, ER Montaldi. 1992. Regulation of the photosynthetic capacity of primary bean leaves by the red: far-red ratio and photosynthetic photon flux density of incident light. Physiol. Plant. 85:97–101.

Hanson HC. 1917. Leaf structure as related to environment. Am. J. Bot. 4:533–560.

Sims, DA, RW Pearcy. 1992. Response of leaf anatomy and photosynthetic capacity in Alocasia macrorrhiza (Araceae) to a transfer from low to high light. Am. J. Bot. 79:449–455.

Akoyunoglou, G, H Anni. 1984. Blue light effect on chloroplast development in higher plants. In: H Senger. (ed.), Blue Light Effects in Biological Systems. Springer-Verlag, Berlin, 397–406.

Boardman NK. 1977. Comparative photosynthesis of sun and shade plants. Ann. Rev. Plant Physiol. 28:355–377.

Cosgrove, DJ. 1981. Rapid suppression of growth by blue light. Plant Physiol. 67: 584–590.

Saebo, A, T Krekling. M Appelgren. 1995. Light quality affects photosynthesis and leaf anatomy of brich plantlets in vitro. Plant Cell Tissue Organ Culture 41:177–185.

Schuerger, AC, C Brown, EC Stryjewski. 1997. Anatomatical Features of Pepper Plants (Capsicum annuum L.) Grown under Red Light-emitting Diodes Supplemented with Blue or Far-red Light. Annuals Bot. 70:273-282.

Senger, H. 1982. The effect of blue light on plants and microorganisms. Phytochem. Photobiol. 35: 911–920.

Tucker, CJ, MW Garrett. 1977. Leaf Optical System modeled as a stochastic process. Applied Optics, 16(3): 635-642.

Halliday KJ, M Koornneef, GC Whitelam. 1994. Phytochrome B and at least one other phytochrome mediate the accelerated flowering response of Arabidopsis thaliana L to low red/far-red ratio. Plant Phys. 104:1311–1315.

Kasperbauer, MJ. 1988. Phytochrome involvement in regulation of the photosynthetic apparatus and plant adaptation. Plant Physiol. Biochem. 26(4):519-524.

Gamon, JA, Surfus, JS. 1999. Assessing leaf pigment content and activity with a reflectometer. New Phtytol. 143:105-117.

Inada, K. 1976. Action spectra for photosynthesis in higher plants. Plant and Cell Phys. 17:355-365.

Almeida, C. C., P. S. Almeida, N. R. Monteiro, M. F. Pinto, and H. A. Braga. 2014. LED-based electronic system to support plant physiology experiments. In Industrial Electronics (ISIE), 2014 IEEE 23rd International Symposium on. IEEE.

Kozai, T. 2012. Sustainable Plant Factory: Closed Plant Production Systems with Artificial Light for High Resource Use Efficiencies and Quality Produce. In International Symposium on Soilless Cultivation 1004.

Kwon, S.-Y., S.-H. Ryu, and J.-H. Lim. 2013. Design and implementation of an integrated management system in a plant factory to save energy. Cluster Computing:1-14.

Hogewoning, S., G. Trouwborst, J. Harbinson, and W. Van Ieperen. 2010a. Light distribution in leaf chambers and its consequences for photosynthesis measurements. Photosynthetica 48(2):219-226.

Hogewoning, S. W., G. Trouwborst, H. Maljaars, H. Poorter, W. van Ieperen, and J. Harbinson. 2010b. Blue light dose–responses of leaf photosynthesis, morphology, and chemical composition of Cucumis sativus grown under different combinations of red and blue light. Journal of Experimental Botany 61(11):3107-3117.

Tamulaitis, G, P Duchovskis, Z Bliznikas, K Breiv, R Ulinskait, A Brazaityte, A Novicˇkovas, AZ Ukauskas 2005. High-power light-emitting diode based facility for plant cultivation. J. Phys. D: Appl. Phys. 38 (2005):3182–3187.

Giacomelli,GA, KC Ting, S Panigrahi. 1987. Solar PAR vs. Solar Total Radiation Transmission in a Greenhouse. Trans. ASABE. 31(5):1540-1543.

Papadopoulus, AP, S Pararajasingham. 1997. The influence of plant spacing on light interception and use in greenhouse tomato (Lycopersicon esculentum Mill): A review. Scientia Horticulturae 69: 1-29.

Massa GD, HH Kim, RM Wheeler, CA Mitchell. 2008. Plant Productivity in Response to LED Lighting. HortScience 43:1951-1956.

Morrow, R. C. 2008. LED lighting in horticulture. HortScience 43(7):1947-1950.

Massa, G., T. Graham, T. Haire, C. Flemming, G. Newsham, and R. Wheeler. 2015. Light-emitting diode light transmission through leaf tissue of seven different crops. HortScience 50(3):501-506.

Yeh, N., and J.-P. Chung. 2009. High-brightness LEDs—Energy efficient lighting sources and their potential in indoor plant cultivation. Renewable and Sustainable Energy Reviews 13(8):2175-2180.

Lefsrud, M. G., D. A. Kopsell, and C. E. Sams. 2008. Irradiance from distinct wavelength light-emitting diodes affect secondary metabolites in kale. HortScience 43(7):2243-2244.

Holonyac, N., S.F. Bevacqua. 1962. Coherent (Visible) Light Emission from Ga(As1-xPx) Junctions. Appl. Phys. Lett. 1:82-83

Lafont, U., H. van Zeijl, and S. van der Zwaag. 2012. Increasing the reliability of solid state lighting systems via self-healing approaches: A review. Microelectronics Reliability 52(1):71-89.

Kasap, S. 2001. PN Junction Devices and Light Emitting Diodes. University of Saskatchewan. Special Custom E-Book. Web February 15, 2013. <http://www.kasap.usask.ca/samples/PNJunctionDevices.pdf>.

Yufeng, L., W. Zhao., Y. Xia., M. Zhu., J. Senawiratne., J. Detchprohm., F. Schubert., C. Wetzel. 2007. Loss of Quantum Efficiency in Green Light Emitting Diode Dies at Low Temperature. Material Research Society Symposium Procedure 955.

Craford M.G. 1992. LEDs challenge the Incandescents. Circuits and Devices Mag., IEEE 8(5):24-29.

Mukai, T., M. Yamada, S. Nakamura. 1999. Characteristics of InGaN-Based UV/Blue/Green/Amber/Red Light-Emitting Diodes. Jpn. J. Appl. Phys.38: 3976–3981.

Xie, W. 1992. Room Temperature Blue Light Emitting p-n Diodes from Zn(S,Se)-Based Multiple Quantum Well Structures. Applied Physics Letters 60 (16):1999-2001.

Steigerwald, D. A., J. C. Bhat., D. Collins., R. M. Fletcher., M. O. Holcomb., M. J. Ludowise., P. S. Martin., S. L. Rudaz. 2002. Illumination with Solid State Lighting Technology. IEEE Journal on Selected Topics in Quantum Electronics, 2 (8): 310-320.

Kim, M. H., M. F. Schubert., Q. Dai., J. K. Kim., E. F. Schubert., J. Piprek., K. Park. 2007. Origin of Efficiency Droop in GaN Based Light-Emitting-Diode. Journal of Applied Physics, 207 (10), 2217-2225.

Nelson, J. A., B. Bugbee. 2013. Supplemental Greenhouse Lighting: Return on Investment for LED and HPS fixtures. Web August 25, 2013.

< http://cpl.usu.edu/files/publications/factsheet/pub 4964212.pdf>

Tsao, J.Y. 2004. Solid State Lighting: Lamps, Chips, and Materials for Tomorrow. IEEE Circuits& Devices Magazine, 3(20), 28-37.

Fu, M., L. Yang, J. Zhang. 2011. Study of Light Emitting Diodes for the Application of Plant Growth in Green House.Intl. Conf. on Elec. Packing Tech. & High Density Packaging 1106-1110.

XiaoYing, L., G. ShiRong, C. TaoTao, X. ZhiGang, J. XueLei. 2012. Regulation of the Growth and Photosynthesis of Cherry Tomato Seedlings by Different Light Irradiations of Light Emitting Diodes (LED). African J. of Biotech. 11(22):6169-6177.

Tsao, J. Y., M. E. Coltrin., M. H. Crawford., J. A. Simmons. 2010. Solid-State Lighting: An Integrated Human Factors Technology and Economic Perspective. Proceedings of the IEEE, 7 (98), 1162- 1179.

Martineau, V., M. Lefsrud., M. T. Naznin., D. A. Kopsell. 2012. Comparison of Light-emitting Diode and High-pressure Sodium Light Treatments for Hydroponics Growth of Boston Lettuce. HortScience, 47(4), 477-482.

Gómez, C., R. C. Morrow, C. M. Bourget, G. D. Massa, and C. A. Mitchell. 2013. Comparison of intracanopy light-emitting diode towers and overhead high-pressure sodium lamps for supplemental lighting of greenhouse-grown tomatoes. HortTechnology 23(1):93-98.

Brown, C s., A.C. Schuerger, J.C. Sager. 1995. Growth and Photomorphogenesis of Pepper Plants Under Red Light-Emitting Diodes with Supplemental Blue or Far-Red Lighting. J. Am. Soc. Hort. Sci. 120:808-813.

Bula, R. J., R. C. Morrow., T. W. Tibbitts., D. J. Barta. 1991. Light Emitting Diodes as a Radiation Source for Plants. HortScience, 26(2), 203-205.

Urbonaviciut, A., P. Pinho., G. Samuolien., P. Duchovskis., P. Vitta., A. Stonkus., G. Tamulaitis, A. Žukauskas ., L. Halonen. 2007. Effect of Short-Wavelength Light on Lettuce Growth and Nutritional Quality. Scientific Works of the Lithuanian Institute of Horticulture and Lithuanian University of Agriculture - Sodininkyst Ir Daržininkyst, (26), 157-165.

Mathieu, J. J., L. D. Albright. 2004. A Stand-Alone Light Integral Controller. Acta Horticulturae, 633, 153-159.

Ieperen, W. V., G. Trouwborst. 2008. The Application of LEDs as Assimilation Light Source in Greenhouse Horticulture: a Simulation Study. Acta Horticulturae, (801), 1407-1414.

Dorais, M. 2003. The Use of Supplemental Lighting for Vegetable Crop Production: Light Intensity, Crop Response, Nutrition, Crop Management, Cultural Practices. Canadian Greenhouse Conference. Toronto, Ontario.

Gu, Y., and N. Narendran. 2004. A noncontact method for determining junction temperature of phosphor-converted white LEDs. In Third international conference on solid state lighting. International Society for Optics and Photonics.

Schanda, J., P. Csuti, and F. Szabó. 2014. Laboratory Measurement of Optical Properties of LEDs. In Thermal Management for LED Applications, 167-196. Springer.

Xi, Y., T. Gessmann, J. Xi, J. K. Kim, J. M. Shah, E. F. Schubert, A. J. Fischer, M. H. Crawford, K. H. Bogart, and A. A. Allerman. 2005a. Junction temperature in ultraviolet light-emitting diodes. Japanese Journal of Applied Physics 44(10R):7260.

Xi, Y., J.-Q. Xi, T. Gessmann, J. Shah, J. Kim, E. Schubert, A. Fischer, M. Crawford, K. Bogart, and A. J. A. p. l. Allerman. 2005b. Junction and carrier temperature measurements in deep-ultraviolet light-emitting diodes using three different methods. 86(3):031907.

Yang, D., and M. Cai. 2013. SSL Case Study: Package, Module, and System. In Solid State Lighting Reliability, 427-453. Springer.

Li, J., J. Wang, Z. Liu, and A. Poppe. 2014. Solid State Physics Fundamentals of LED Thermal Behavior. In Thermal Management for LED Applications, 15-52. Springer.

Li, K., Z. Li, and Q. Yang. 2016. Improving light distribution by zoom lens for electricity savings in a plant factory with light-emitting diodes. Frontiers in plant science 7:92.

Peng, L.-H., C.-W. Chuang, and L.-H. Lou. 1999. Piezoelectric effects in the optical properties of strained InGaN quantum wells. Applied physics letters 74(6):795-797.

Chang, M.-H., D. Das, P. Varde, and M. Pecht. 2012. Light emitting diodes reliability review. Microelectronics Reliability 52(5):762-782.

Liu, J., W.-S. Tam, H. Wong, and V. Filip. 2009. Temperature-dependent light-emitting characteristics of InGaN/GaN diodes. Microelectronics Reliability 49(1):38-41.

Christensen, A., and S. Graham. 2009. Thermal effects in packaging high power light emitting diode arrays. Applied Thermal Engineering 29(2):364-371.

Su, Y.-F., S.-Y. Yang, T.-Y. Hung, C.-C. Lee, and K.-N. Chiang. 2012. Light degradation test and design of thermal performance for high-power light-emitting diodes. Microelectronics Reliability 52(5):794-803.

McCartney, L., and M. Lefsrud. 2018. Protected agriculture in extreme environments: A review of controlled environment agriculture in tropical, arid, polar and urban locations. Applied Engineering in Agriculture 34(2):455-473.

Langhans, R. W., and T. Tibbitts. 1997. Plant growth chamber handbook.

Cole, M., and T. Driscoll. 2014. The lighting revolution: If we were experts before, we're novices now. IEEE Transactions on Industry Applications 50(2):1509-1520.

Poulet, L., G. Massa, R. Morrow, C. Bourget, R. Wheeler, and C. A. Mitchell. 2014. Significant reduction in energy for plant-growth lighting in space using targeted LED lighting and spectral manipulation. Life Sciences in Space Research 2:43-53.

Both, A.-J., B. Bugbee, C. Kubota, R. G. Lopez, C. Mitchell, E. S. Runkle, and C. Wallace. 2017. Proposed product label for electric lamps used in the plant sciences. HortTechnology 27(4):544-549.

Both, A., D. Ciolkosz, and L. Albright. 2000. Evaluation of light uniformity underneath supplemental lighting systems. In IV International ISHS Symposium on Artificial Lighting 580.

Gómez, C., and C. A. Mitchell. 2015. Growth responses of tomato seedlings to different spectra of supplemental lighting. HortScience 50(1):112-118.

Magagnini, G., G. Grassi, and S. Kotiranta. 2018. The effect of light spectrum on the morphology and cannabinoid content of Cannabis sativa L. Medical Cannabis and Cannabinoids 1(1):19-27.

Nelson, J. A., and B. Bugbee. 2014. Economic analysis of greenhouse lighting: light emitting diodes vs. high intensity discharge fixtures. PloS one 9(6):e99010.

Wallace, C., and A. Both. 2016. Evaluating operating characteristics of light sources for horticultural applications. In VIII International Symposium on Light in Horticulture 1134.

Chen, W.-C., T.-T. Lai, M.-W. Wang, and H.-W. Hung. 2011. An optimization system for LED lens design. Expert Systems with Applications 38(9):11976-11983.

Whang, A. J.-W., Y.-Y. Chen, and Y.-T. Teng. 2009. Designing uniform illumination systems by surface-tailored lens and configurations of LED arrays. Journal of display technology 5(3):94-103.

Ciolkosz, D., L. Albright, J. Sager, and R. Langhans. 2002. A model for plant lighting system selection. Transactions of the ASAE 45(1):215.

Ciolkosz, D., A. Both, and L. Albright. 2001. Selection and placement of greenhouse luminaires for uniformity. Applied Engineering in Agriculture 17(6):875.

King, S. 2008. Luminous intensity of an LED as a function of input power. International School Bangkok Journal of Physics, v. 2, 06 2008.

Yung, K. C., Liem, H., & Choy, H. S. (2013). Heat dissipation performance of a high-brightness LED package assembly using high-thermal conductivity filler. Applied optics, 52(35), 8484–8493.

Scheer H (2006). "An Overview of Chlorophylls and Bacteriochlorophylls: Biochemistry, Biophysics, Functions and Applications". Chlorophylls and Bacteriochlorophylls. Advances in Photosynthesis and Respiration. Vol. 25. pp. 1–26.

Vershinin, Alexander (1999-01-01). "Biological functions of carotenoids - diversity and evolution". BioFactors. 10 (2–3): 99–104.

Cogdell, R. J. (1978-11-30). "Carotenoids in photosynthesis". Phil. Trans. R. Soc. Lond. B. 284 (1002): 569–579.

Merzlyak MN, Chivkunova OB, Maslova IP, Naqvi KR, Solovchenko AE, Klyachko-Gurvich GL (2008) Light absorption and scattering by cell suspensions of some cyanobacteria and microalgae. Russ J Plant Physiol 55(3):420–425. https:// doi. org/ 10. 1134/ S1021 4437080301 99

John R. D. Hervey, Paolo Bombelli, David J. Lea‐Smith, Alan K. Hulme, Nathan R. Hulme, Atvinder K. Rullay, Robert Keighley, Christopher J. Howe (2021). “A dual compartment cuvette system for correcting scattering in whole‐cell absorbance spectroscopy of photosynthetic microorganisms”. Springer Nature.

Anastasia A. Lykina, Dmitry N. Artemyev, and Ivan A. Bratchenko. “Analysis of albumin Raman scattering registration efficiency from different volume and shape cuvette” (2017). Journal of Biomedical Photonics & Engineering · May 2017 DOI: 10.18287/JBPE17.03.020309

Sonia E. Evans, Peter Duggan, Matthew E. Bergman , Daniela Cobo‐López, Benjamin Davis,

Ibadat Bajwa and Michael A. Phillips (2022). “Design and fabrication of an improved dynamic flow cuvette for 13CO2 labeling in Arabidopsis plants”. Evans et al. Plant Methods (2022) 18:40 https://doi.org/10.1186/s13007-022-00873-3

Merzlyak MN, Naqvi KR (2000) On recording the true absorption spectrum and the scattering spectrum of a turbid sample: application to cell suspensions of the cyanobacterium Anabaena variabilis. J Photochem Photobiol B 58(2–3):123–129. https:// doi. org/ 10. 1016/ S1011-1344(00) 00114-7

Jackson SA, Hervey JRD, Dale AJ, Eaton-Rye JJ (2014) Removal of both Ycf48 and Psb27 in Synechocystis sp. PCC 6803 disrupts Photosystem II assembly and alters Q A − oxidation in the mature complex. FEBS Lett 588(20):3751–3760. https:// doi. org/ 10. 1016/j. febsl et. 2014. 08. 024

Tarun, Agarwal (24 October 2013). "Stepper Motor – Types, Advantages & Applications" https://www.elprocus.com/stepper-motor-types-advantages-applications/

Dill, Lawrence M. (1977). "Refraction and the spitting behavior of the archerfish (Toxotes chatareus)". Behavioral Ecology and Sociobiology. 2 (2): 169–184.

Jenkins & White. Fundamentals of optics. 4th ed., McGraw-Hill, 1976.

Gloge, D. (1 October 1971). "Weakly Guiding Fibers". Applied Optics. 10 (10): 2252–8.

J. Hecht: Understanding Fiber Optics, Ch. 1-3, Prentice Hall N.J. 1999

D. R. Goff: Fiber Optic Reference Guide (2nd ed.) Focal Press 1999

Zajac, Alfred; Hecht, Eugene (18 March 2003). Optics, Fourth Edit. Pearson Higher Education.

https://emadrlc.blogspot.com/2013/01/stepper-motor-construction.html

https://www.physics-and-radio-electronics.com/electronic-devices-and-circuits/semiconductor-diodes/forwardbiasedpnjunctionsemiconductordiode.html

Appendix

The below figures demonstrate the transmittance results obtained from the tests. The vertical axis denotes the relative spectral transmittance, while the horizontal axis denotes the wavelength in nm.

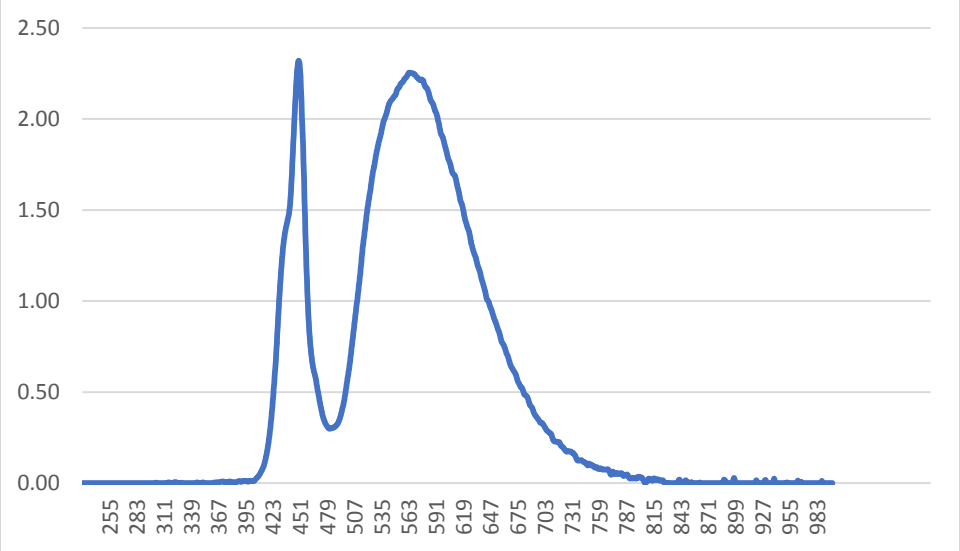

Figure A30: White LED (oil 0°) cylindrical cuvette

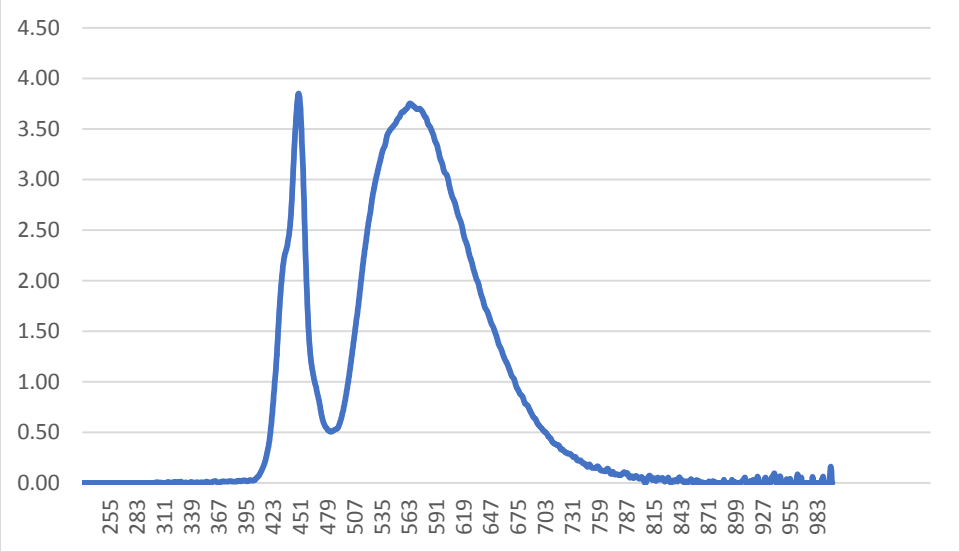

Figure A31: White LED (oil 1 step) cylindrical cuvette, a step is 3° 45'

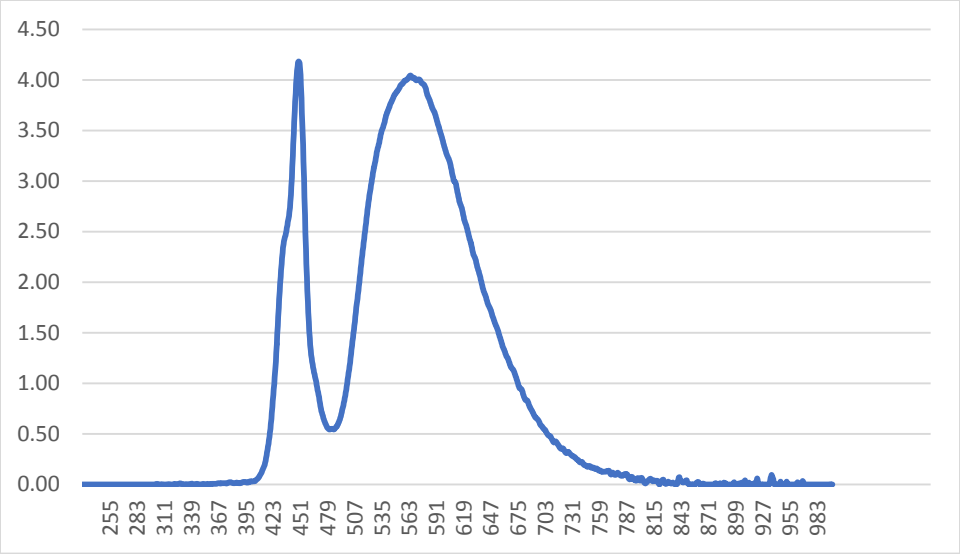

Figure A32: White LED (oil 2 steps) cylindrical cuvette, a step is 3° 45'

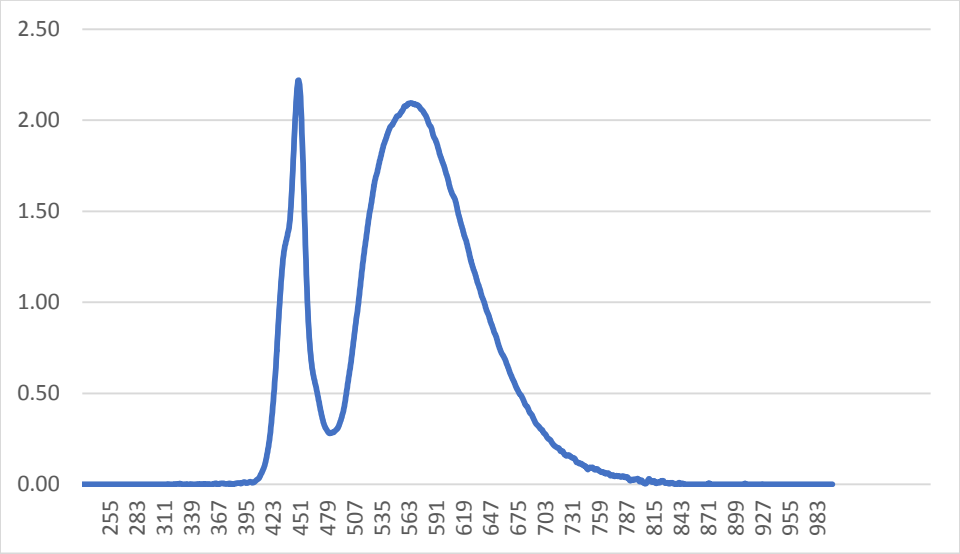

Figure A33: White LED (oil 3 steps) cylindrical cuvette, a step is 3° 45'

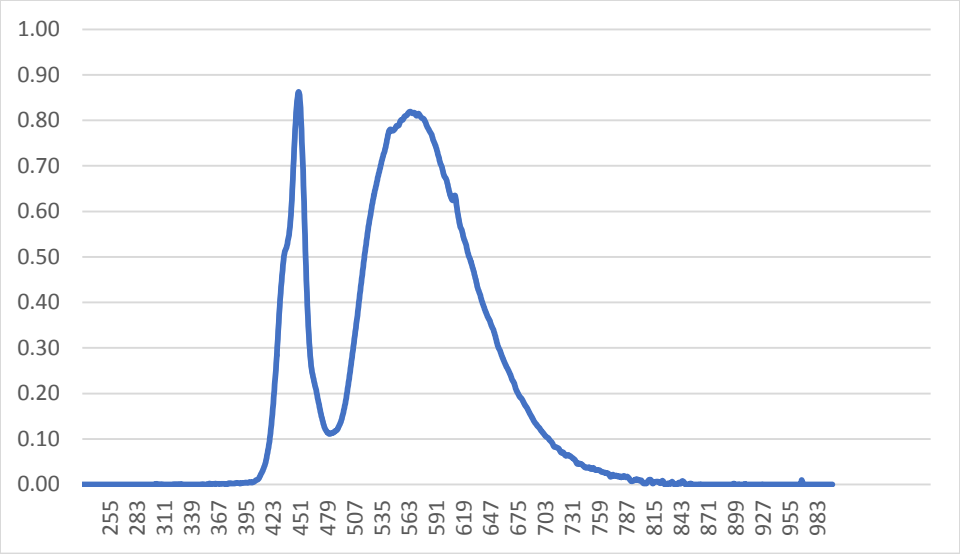

Figure A34: White LED (oil 4 steps) cylindrical cuvette, a step is 3° 45'

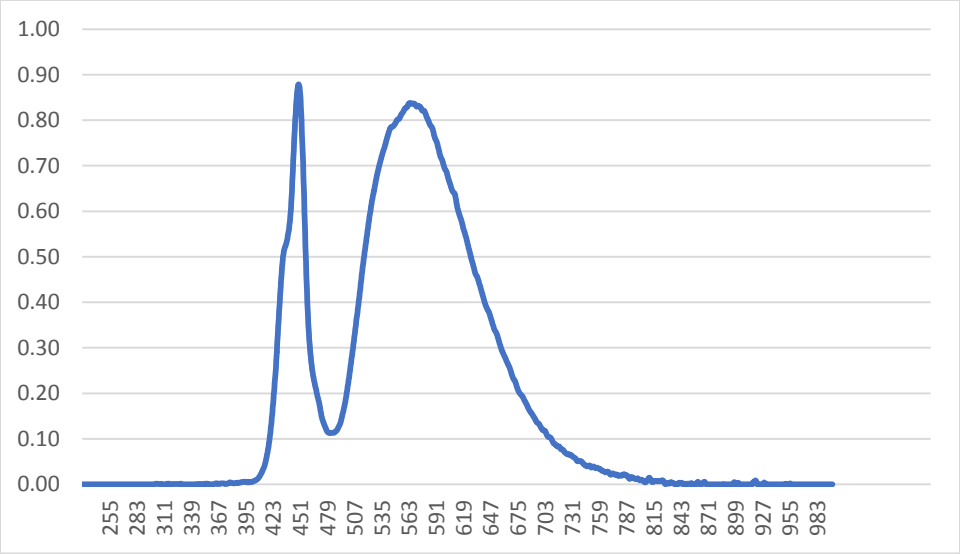

Figure A35: White LED (oil 90°) cylindrical cuvette

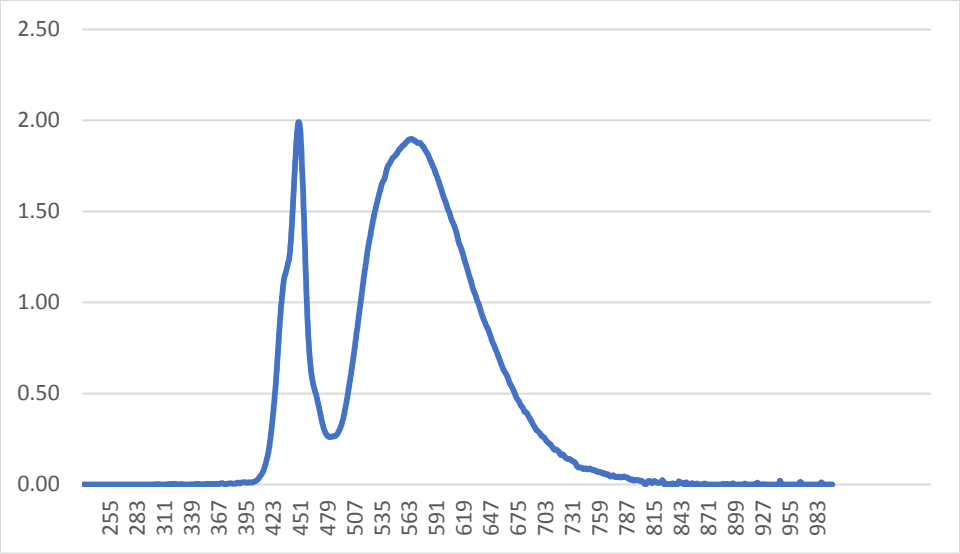

Figure A36: White LED (water 0°) cylindrical cuvette

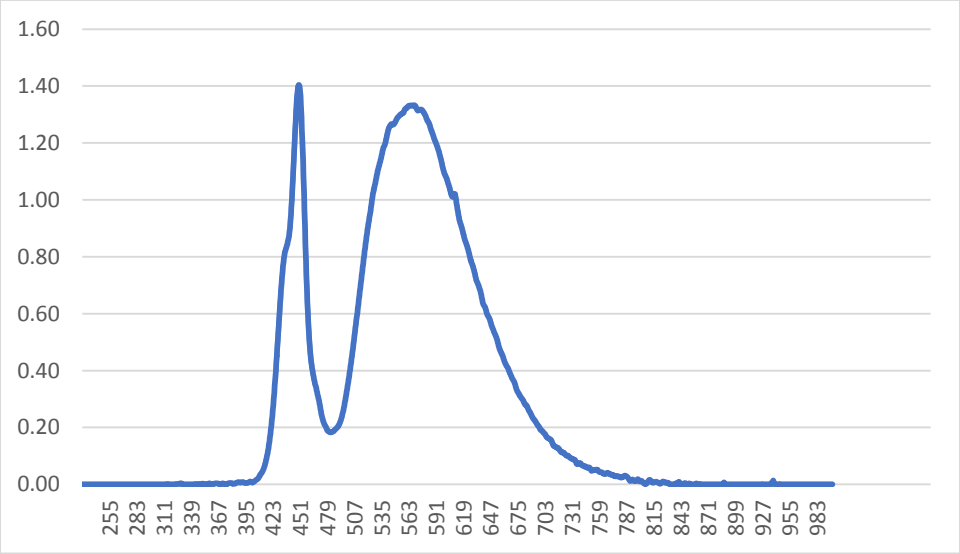

Figure A37: White LED (water 1 step) cylindrical cuvette, a step is 3° 45'

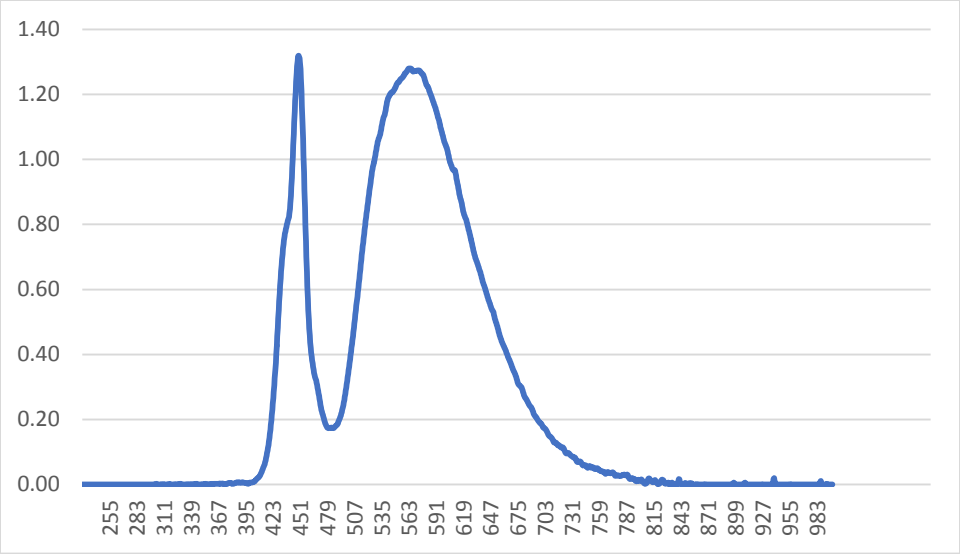

Figure A38: White LED (water 2 steps) cylindrical cuvette, a step is 3° 45'

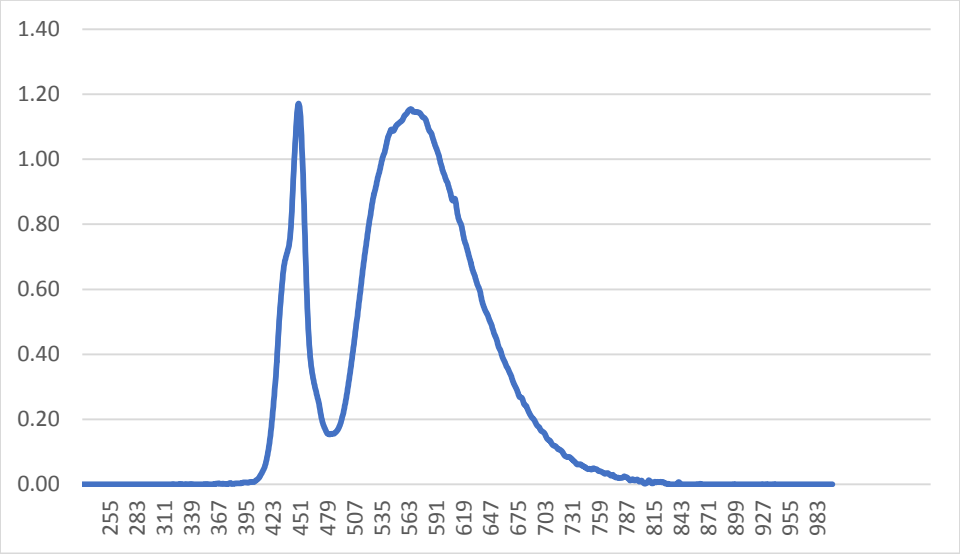

Figure A39: White LED (water 3 steps) cylindrical cuvette, a step is 3° 45'

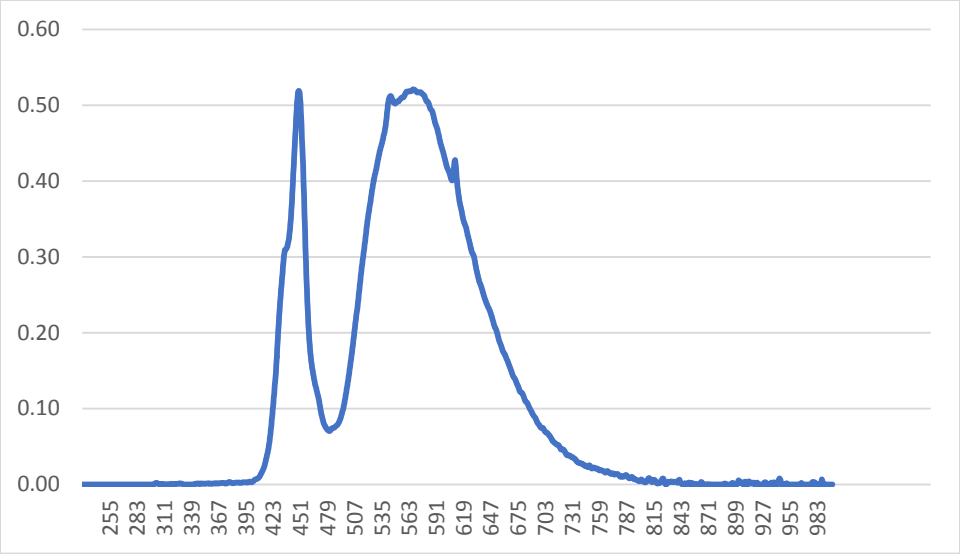

Figure A40: White LED (water 4 steps) cylindrical cuvette, a step is 3° 45'

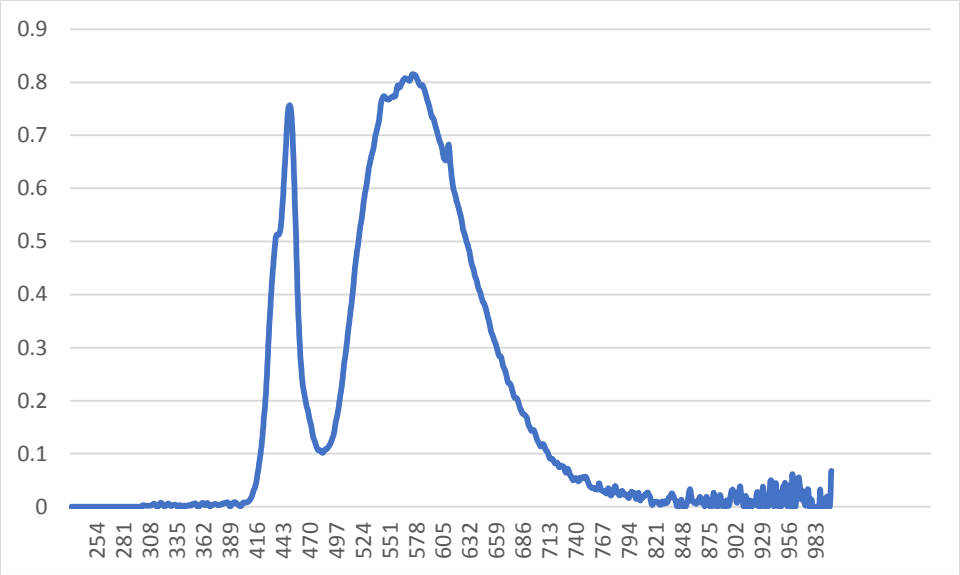

Figure A41: White LED (water 90°) cylindrical cuvette

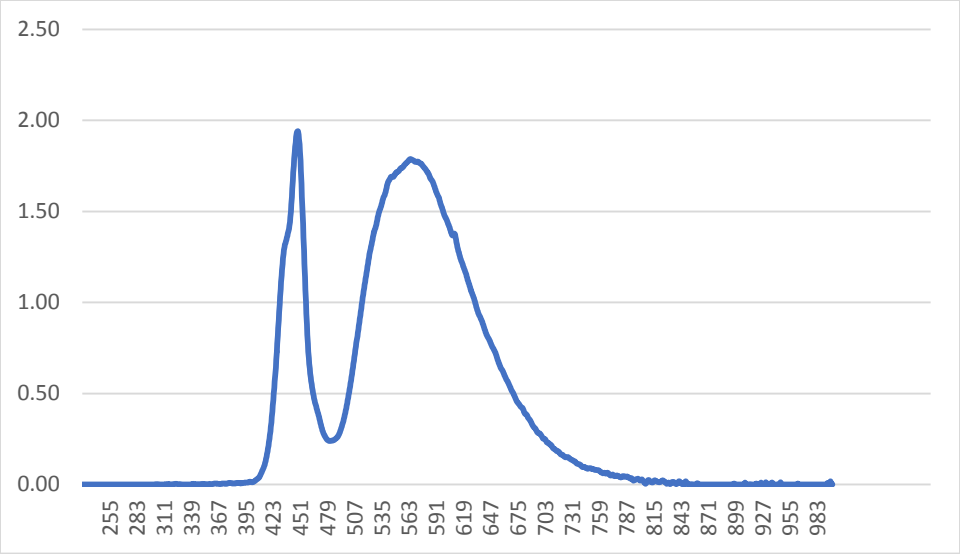

Figure A42: White LED (oil 0°) rectangular cuvette

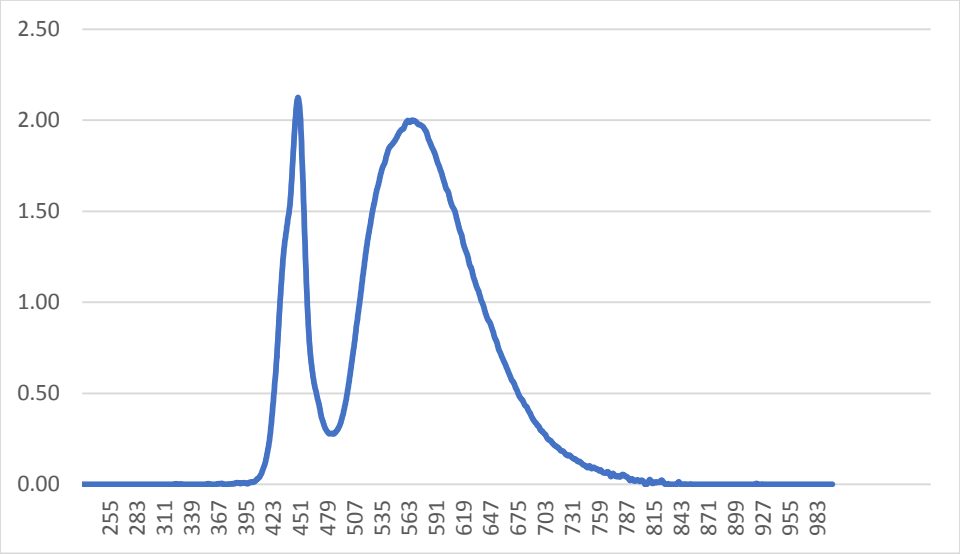

Figure A43: White LED (oil 1 step) rectangular cuvette, a step is 3° 45'

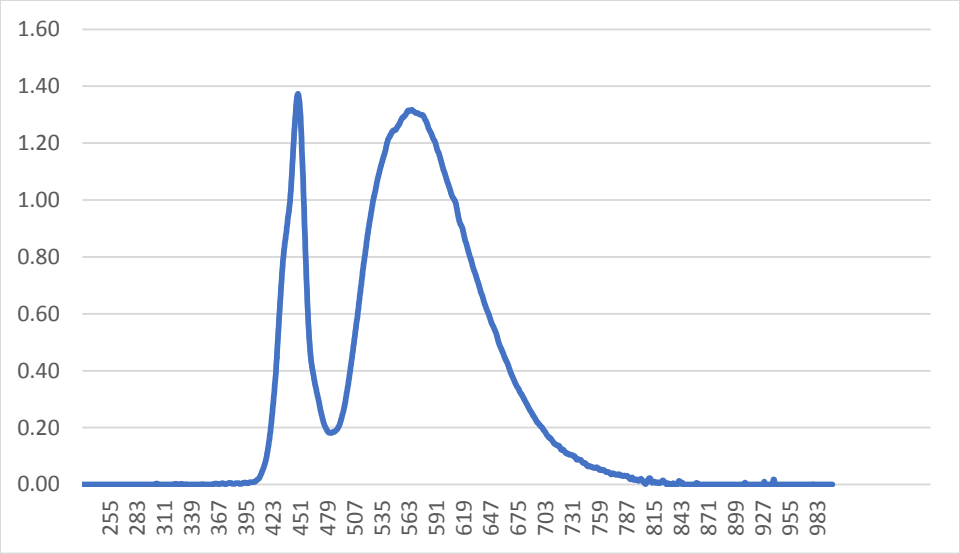

Figure A44: White LED (oil 2 steps) rectangular cuvette, a step is 3° 45'

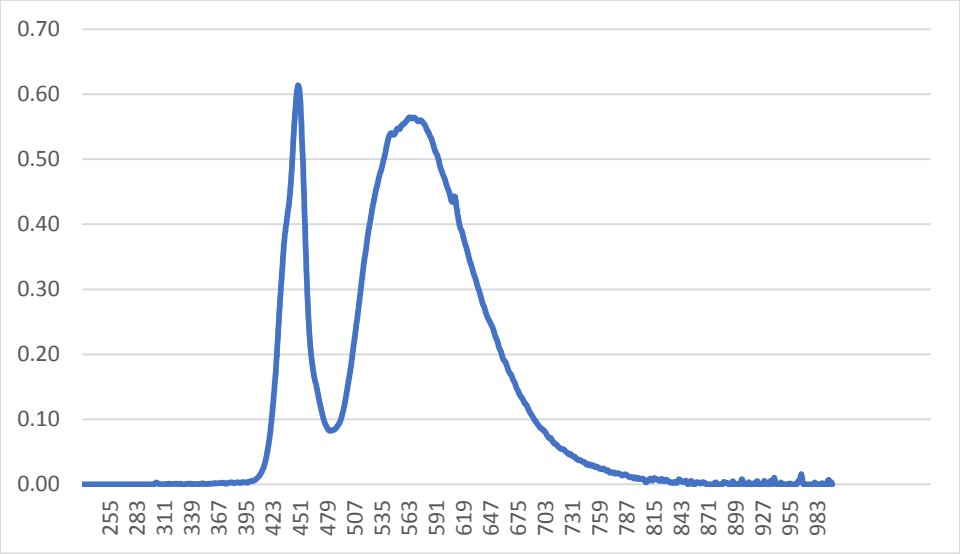

Figure A45: White LED (oil 3 steps) rectangular cuvette, a step is 3° 45'

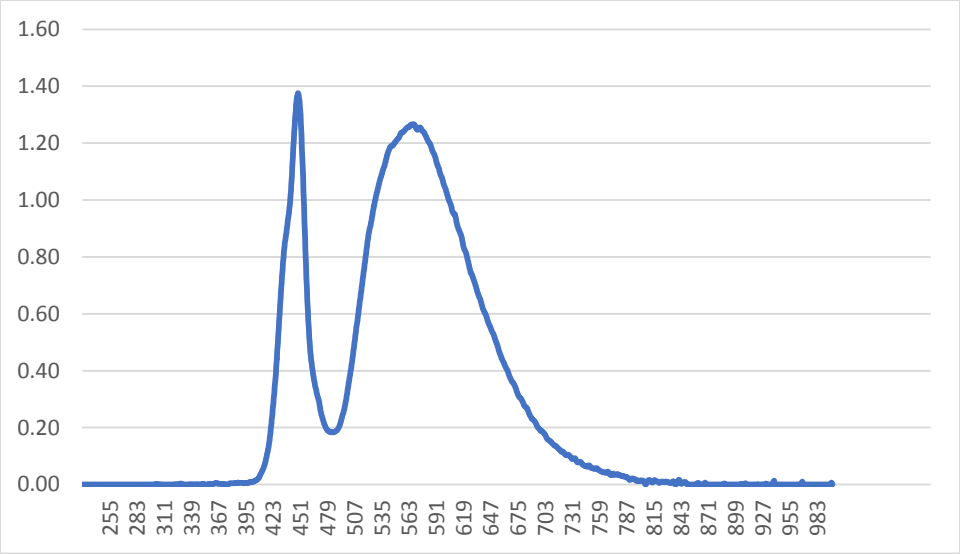

Figure A46: White LED (oil 4 steps) rectangular cuvette, a step is 3° 45'

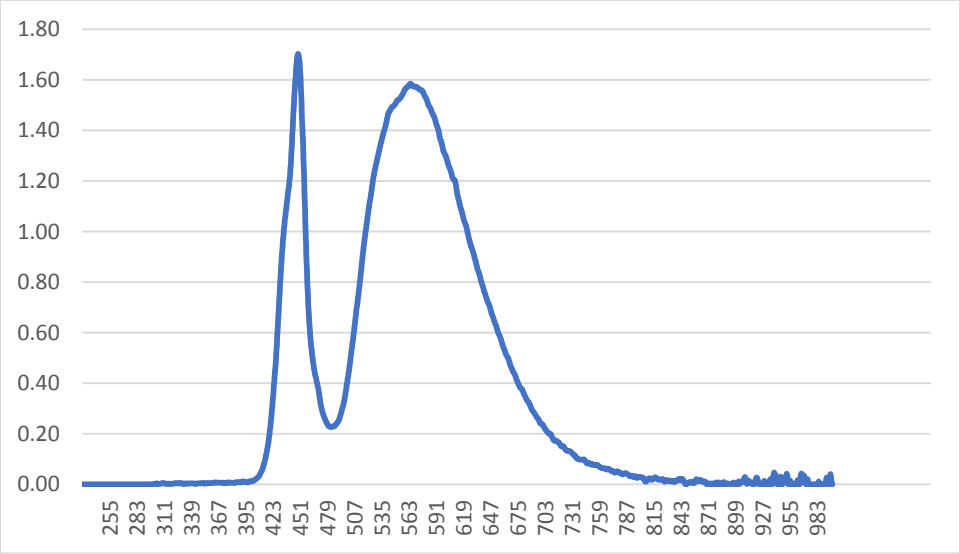

Figure A47: White LED (oil 90°) rectangular cuvette

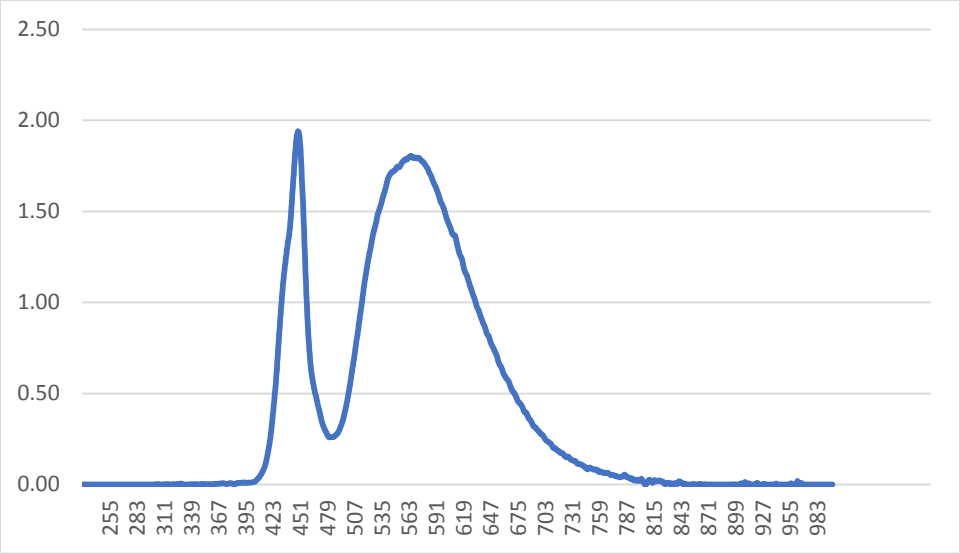

Figure A48: White LED (water 0°) rectangular cuvette

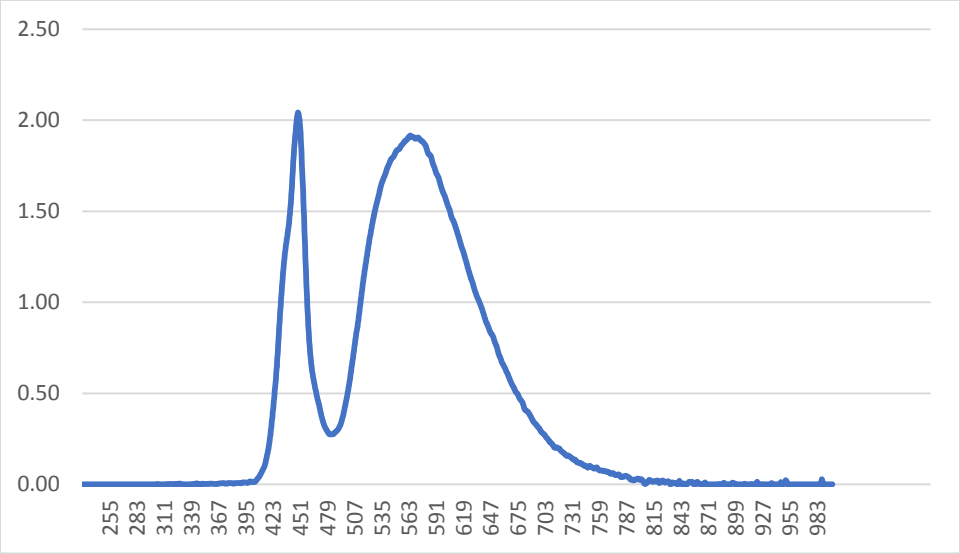

Figure A49: White LED (water 1 step) rectangular cuvette, a step is 3° 45'

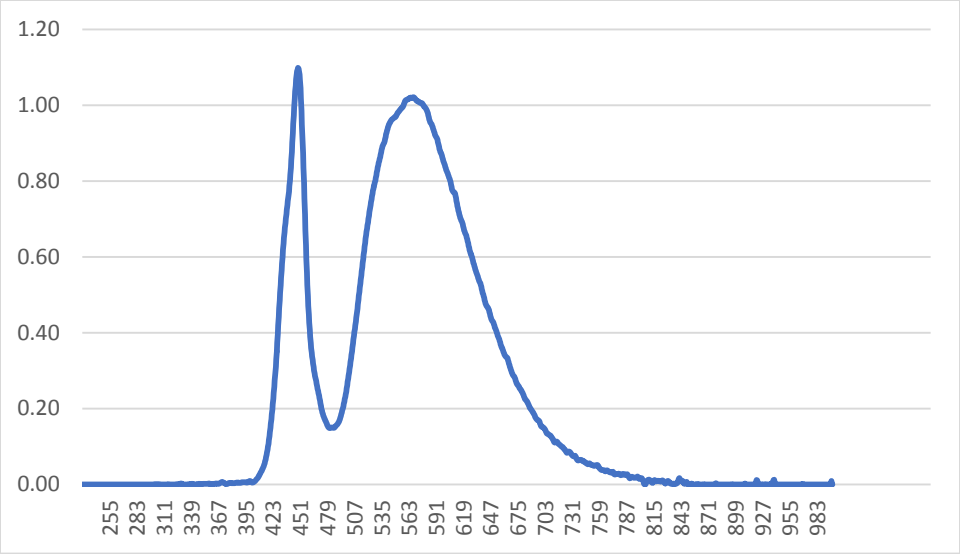

Figure A50: White LED (water 2 steps) rectangular cuvette, a step is 3° 45'

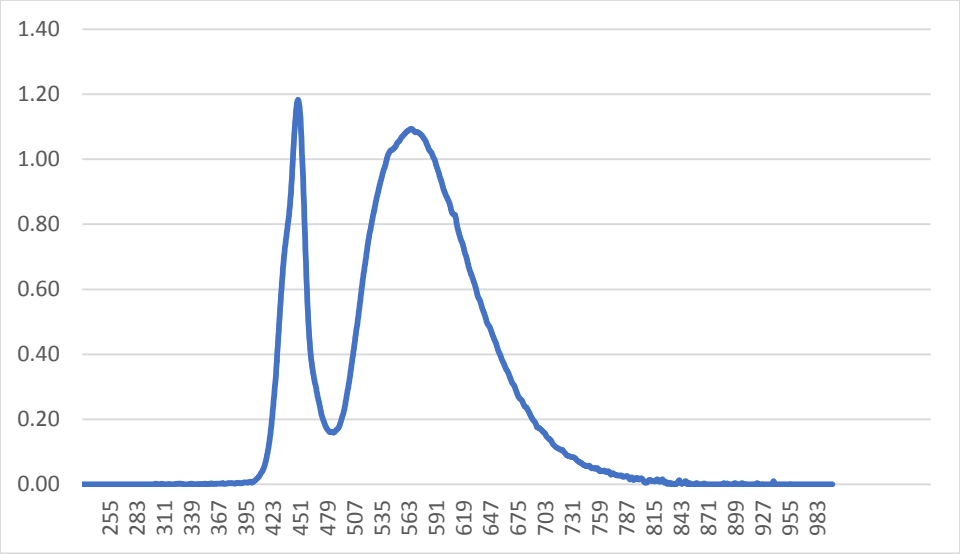

Figure A51: White LED (water 3 steps) rectangular cuvette, a step is 3° 45'

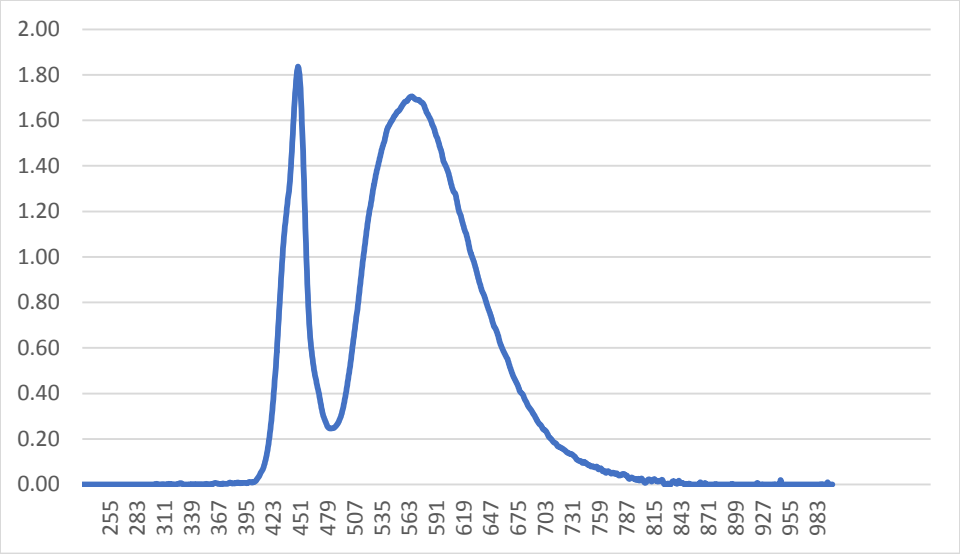

Figure A52: White LED (water 4 steps) rectangular cuvette, a step is 3° 45'

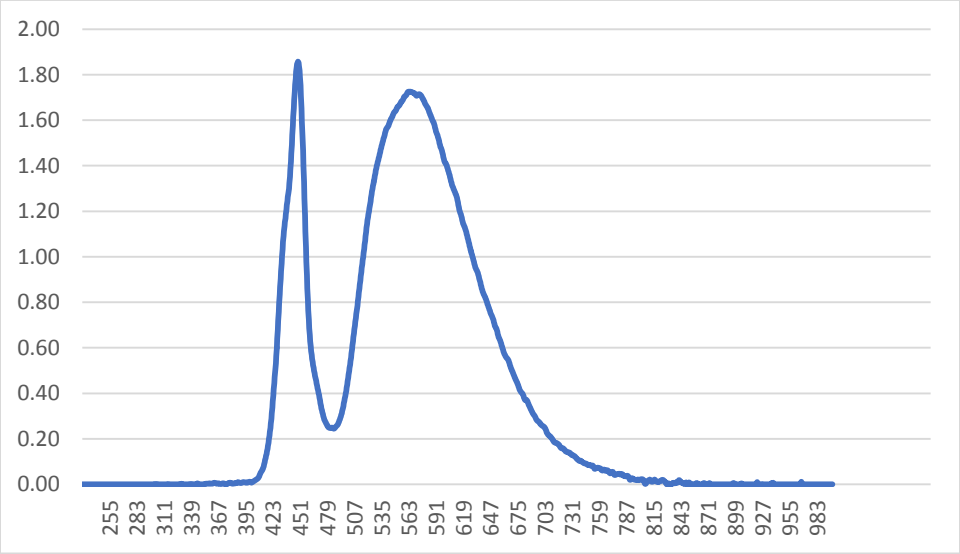

Figure A53: White LED (water 90°) rectangular cuvette